DNA synthesis assay. DNA synthesis was measured by performing a BrdU incorporation assay with a commercially available kit (Roche) as directed by the manufacturer. Cardiomyocyte-conditioned medium was collected as previously described (43). Briefly, cultured cardiomyocytes were starved in DMEM without FBS and were pretreated with EPO (10 U/ml) or saline for 48 hours, and then the medium was collected and transferred to HUVECs. HUVECs were plated in 96-well plates at a density of 5×10^4 cells/well in endothelial cell basal medium-2 with EGM-2 Bullet Kit (Cambrex) for 8 hours and then switched to cardiomyocyte-conditioned medium for 12 hours. BrdU was added to the medium, and BrdU incorporation was detected by ELISA using anti-BrdU antibody. VEGF receptor antagonist CBO-P11 (44, 45) (12 μM; Calbiochem) and anti–Ang-1 antibody (1 μg/ml; Chemicon) were used for the inhibition studies.

Tube formation assay. Matrigel (growth factor reduced, 100 μl; BD Biosciences) was added to each well of a 48-well plate and allowed to polymerize at 37°C for 1 hour. HUVECs (1×10^4) were seeded onto Matrigel in endothelial cell basal medium-2 with EGM-2 Bullet Kit and cultured for 1 hour and then switched to cardiomyocyte-conditioned medium described above. After 8 hours, tube length was quantified using an angiogenesis image analyzer (Kurabo).

Isolated heart perfusion system. Isolated heart perfusion system was used to measure coronary flow as previously described (46). In brief, mouse hearts were excised rapidly and mounted on a Langendorff perfusion system. All isolated hearts were stabilized by perfusion of Krebs-Henseleit buffer, and perfusion pressure was adjusted to 60 mmHg. The heart was paced at 400 bpm. After an adjustment period, the coronary effluent was collected and the coronary flow was calculated. After baseline measurements, sodium nitroprusside (10^{-4} M, Sigma-Aldrich) was infused into the perfusate, and coronary flow was measured.

Statistics. All data are shown as mean ± SEM. Multiple group comparison was performed by 1-way ANOVA followed by Bonferroni's procedure for comparison of means. Comparison between 2 groups was analyzed by the 2-tailed Student's *t* test. Values of $P < 0.05$ were considered statistically significant.

Acknowledgments

The authors thank M. Yamamoto (Tohoku University School of Medicine, Miyagi, Japan) for generously providing RES mice. The authors thank Y. Ohtsuki, M. Ikeda, I. Sakamoto, A. Furuyama, M. Kikuchi, and H. Maruyama for their excellent technical assistance. This work was supported by a Grant-in-Aid for Scientific Research from the Ministry of Education, Science, Sports, and Culture, and Health and Labor Sciences research grants (to I. Komuro) and a Grant-in-Aid for Scientific Research from the Ministry of Education, Culture, Sports, Science and Technology of Japan and grants from the Terumo Life Science Foundation (to H. Takano).

Received for publication May 18, 2009, and accepted in revised form March 24, 2010.

Address correspondence to: Issei Komuro, Department of Cardiovascular Science and Medicine, Chiba University Graduate School of Medicine, 1-8-1 Inohana, Chuo-ku, Chiba 260-8670, Japan. Phone: 81.43.226.2097; Fax: 81.43.226.2557; E-mail: komuro-tky@umin.ac.jp.

1. Jessup M, Brozena S. Heart failure. *N Engl J Med.* 2003;348(20):2007–2018.
2. Rosamond W, et al. Heart disease and stroke statistics--2008 update: a report from the American Heart Association Statistics Committee and Stroke Statistics Subcommittee. *Circulation.* 2008;117(4):e25–146.
3. Moon C, et al. Erythropoietin reduces myocardial infarction and left ventricular functional decline after coronary artery ligation in rats. *Proc Natl Acad Sci U S A.* 2003;100(20):11612–11617.
4. Ohtsuka M, et al. Cytokine therapy prevents left ventricular remodeling and dysfunction after myocardial infarction through neovascularization. *FASEB J.* 2004;18(7):851–853.
5. Harada M, et al. G-CSF prevents cardiac remodeling after myocardial infarction by activating the Jak-Stat pathway in cardiomyocytes. *Nat Med.* 2005;11(3):305–311.
6. Silverberg DS, et al. The effect of correction of mild anemia in severe, resistant congestive heart failure using subcutaneous erythropoietin and intravenous iron: a randomized controlled study. *J Am Coll Cardiol.* 2001;37(7):1775–1780.
7. Ponikowski P, et al. Effect of darbepoetin alfa on exercise tolerance in anemic patients with symptomatic chronic heart failure: a randomized, double-blind, placebo-controlled trial. *J Am Coll Cardiol.* 2007;49(7):753–762.
8. Felker GM, Adams KF Jr, Gattis WA, O'Connor CM. Anemia as a risk factor and therapeutic target in heart failure. *J Am Coll Cardiol.* 2004;44(5):959–966.
9. Bahlmann FH, et al. Erythropoietin regulates endothelial progenitor cells. *Blood.* 2004; 103(3):921–926.
10. Parsa C, et al. A novel protective effect of erythropoietin in the infarcted heart. *J Clin Invest.* 2003; 112(7):999–1007.
11. Wright GL, Hanlon P, Amin K, Steenbergen C, Murphy E, Arcasoy MO. Erythropoietin receptor expression in adult rat cardiomyocytes is associated with an acute cardioprotective effect for recombinant erythropoietin during ischemia-reperfusion injury. *FASEB J.* 2004;18(9):1031–1033.
12. Brines M, Cerami A. Emerging biological roles for erythropoietin in the nervous system. *Nat Rev Neurosci.* 2005;6(6):484–494.
13. Tada H, et al. Endogenous erythropoietin system in non-hematopoietic lineage cells plays a protective role in myocardial ischemia/reperfusion. *Cardiovasc Res.* 2006;71(3):466–477.
14. Asaumi Y, et al. Protective role of endogenous erythropoietin system in nonhematopoietic cells against pressure overload-induced left ventricular dysfunction in mice. *Circulation.* 2007;115(15):2022–2032.
15. Suzuki N, et al. Erythroid-specific expression of the erythropoietin receptor rescued its null mutant mice from lethality. *Blood.* 2002;100(7):2279–2288.
16. Li Y, et al. Reduction of inflammatory cytokine expression and oxidative damage by erythropoietin in chronic heart failure. *Cardiovasc Res.* 2006;71(4):684–694.
17. Hirose S, et al. Erythropoietin attenuates the development of experimental autoimmune myocarditis. *Cardiovasc Drugs Ther.* 2007;21(1):17–27.
18. Abbate A, Biondi-Zoccai GG, Baldi A. Pathophysiologic role of myocardial apoptosis in post-infarction left ventricular remodeling. *J Cell Physiol.* 2002;193(2):145–153.
19. Latini R, Brines M, Fiordaliso F. Do non-hemopoietic effects of erythropoietin play a beneficial role in heart failure? *Heart Fail Rev.* 2008;13(4):415–423.
20. Pagès G, Pouysségur J. Transcriptional regulation of the Vascular Endothelial Growth Factor gene--a concert of activating factors. *Cardiovasc Res.* 2005;65(3):564–573.
21. Wang L, et al. The sonic hedgehog pathway mediates carbamylated erythropoietin–enhanced proliferation and differentiation of adult neural progenitor cells. *J Biol Chem.* 2007;282(42):32462–32470.
22. Pola R, et al. The morphogen sonic hedgehog is an indirect angiogenic agent upregulating two families of angiogenic growth factors. *Nat Med.* 2001;7(6):706–711.
23. Kusano KF, et al. Sonic hedgehog myocardial gene therapy: tissue repair through transient reconstitution of embryonic signaling. *Nat Med.* 2005;11(11):1197–1204.
24. Washington Smoak I, et al. Sonic hedgehog is required for cardiac outflow tract and neural crest cell development. *Dev Biol.* 2005;283(2):357–372.
25. Lewis PM, et al. Cholesterol modification of sonic hedgehog is required for long-range signaling activity and effective modulation of signaling by Ptc1. *Cell.* 2001;105(5):599–612.
26. Sohal DS, et al. Temporally regulated and tissue-specific gene manipulations in the adult and embryonic heart using a tamoxifen-inducible Cre protein. *Circ Res.* 2001;89(1):20–25.
27. Suri C, et al. Increased vascularization in mice overexpressing angiopoietin-1. *Science.* 1998; 282(5388):468–471.
28. Asahara T, et al. Tie2 receptor ligands, angiopoietin-1 and angiopoietin-2, modulate VEGF-induced postnatal neovascularization *Circ Res.* 1998;83(3):233–240.
29. Holash J, Wiegand SJ, Yancopoulos GD. New model of tumor angiogenesis: dynamic balance between vessel regression and growth mediated by angiopoietins and VEGF. *Oncogene.* 1999;18(38):5356–5362.
30. Sano M, et al. p53-induced inhibition of Hif-1 causes cardiac dysfunction during pressure overload. *Nature.* 2007;446(7134):444–448.
31. Giordano FJ, et al. A cardiac myocyte vascular endothelial growth factor paracrine pathway is required to maintain cardiac function. *Proc Natl Acad Sci U S A.* 2001;98(10):5780–5785.
32. Lavine KJ, Kovacs A, Ornitz DM. Hedgehog signaling is critical for maintenance of the adult coronary vasculature in mice. *J Clin Invest.* 2008;118(7):2404–2414.
33. Androutsellis-Theotokis A, et al. Notch signaling regulates stem cell numbers in vitro and in vivo. *Nature.* 2006;442(7104):823–826.
34. Kasperczyk H, Baumann B, Debatin KM, Fulda S. Characterization of sonic hedgehog as a novel

NF-kappaB target gene that promotes NF-kappaB-mediated apoptosis resistance and tumor growth in vivo. *FASEB J.* 2009;23(1):21–33.
35. Digicaylioglu M, Lipton SA. Erythropoietin-mediated neuroprotection involves cross-talk between Jak2 and NF-kappaB signalling cascades. *Nature.* 2001;412(6847):641–647.
36. Funamoto M, et al. Signal transducer and activator of transcription 3 is required for glycoprotein 130–mediated induction of vascular endothelial growth factor in cardiac myocytes. *J Biol Chem.* 2000;275(14):10561–10566.
37. Kendall RL, Thomas KA. Inhibition of vascular endothelial cell growth factor activity by an endogenously encoded soluble receptor. *Proc Natl Acad Sci U S A.* 1993;90(22):10705–10709.
38. Nakamura Y, Komatsu N, Nakauchi H. A truncated erythropoietin receptor that fails to prevent programmed cell death of erythroid cells. *Science.* 1992;257(5073):1138–1141.
39. Leucht C, Stigloher C, Wizenmann A, Klafke R, Folchert A, Bally-Cuif L. MicroRNA-9 directs late organizer activity of the midbrain-hindbrain boundary. *Nat Neurosci.* 2008;11(6):641–648.
40. Taipale J, et al. Effects of oncogenic mutations in Smoothened and Patched can be reversed by cyclopamine. *Nature.* 2000;406(6799):1005–1009.
41. Berman D, et al. Medulloblastoma growth inhibition by hedgehog pathway blockade. *Science.* 2002;297(5586):1559–1561.
42. Watkins DN, Berman DM, Burkholder SG, Wang B, Beachy PA, Baylin SB. Hedgehog signalling within airway epithelial progenitors and in small-cell lung cancer. *Nature.* 2003;422(6929):313–317.
43. Zhang Y, Pasparakis M, Kollias G, Simons M. Myocyte-dependent regulation of endothelial cell syndecan-4 expression. Role of TNF-alpha. *J Biol Chem.* 1999;274(8):4786–4790.
44. Zilberberg L, et al. Structure and inhibitory effects on angiogenesis and tumor development of a new vascular endothelial growth inhibitor. *J Biol Chem.* 2003;278(37):35564–35573.
45. Heineke J, et al. Cardiomyocyte GATA4 functions as a stress-responsive regulator of angiogenesis in the murine heart. *J Clin Invest.* 2007;117(11):3198–3210.
46. Bendall J, et al. C. Strain-dependent variation in vascular responses to nitric oxide in the isolated murine heart. *J Mol Cell Cardiol.* 2002;34(10):1325–1333.

Journal of Molecular and Cellular Cardiology 48 (2010) 1280–1289

Contents lists available at ScienceDirect

Journal of Molecular and Cellular Cardiology

journal homepage: www.elsevier.com/locate/yjmcc

Original article

X-box binding protein 1 regulates brain natriuretic peptide through a novel AP1/CRE-like element in cardiomyocytes

Tamaki Sawada [a], Tetsuo Minamino [a,*], Hai Ying Fu [a], Mitsutoshi Asai [a], Keiji Okuda [a], Tadashi Isomura [b], Satoru Yamazaki [c], Yoshihiro Asano [a], Ken-ichiro Okada [a], Osamu Tsukamoto [d], Shoji Sanada [d], Hiroshi Asanuma [e], Masanori Asakura [d], Seiji Takashima [a], Masafumi Kitakaze [d], Issei Komuro [a]

[a] Department of Cardiovascular Medicine, Osaka University Graduate School of Medicine, Suita, Osaka 565-0871, Japan
[b] Department of Cardiovascular Surgery, Hayama Heart Center, 1898 Shimoyamaguchi, Hayama, Kanagawa 240-0116, Japan
[c] Department of Cardiovascular Dynamics, National Cardiovascular Center, Suita, Osaka 565-8565, Japan
[d] Department of Cardiovascular Medicine, National Cardiovascular Center, Suita, Osaka 565-8565, Japan
[e] Department of Emergency Room Medicine, Kinki University School of Medicine, Sayama, Osaka 589-8511, Japan

ARTICLE INFO

Article history:
Received 4 October 2009
Received in revised form 2 February 2010
Accepted 3 February 2010
Available online 17 February 2010

Keywords:
Endoplasmic reticulum
Unfolded protein response
XBP1
Brain natriuretic peptide
AP1/CRE-like element
Transcriptional regulation

ABSTRACT

The unfolded protein response (UPR) is triggered to assist protein folding when endoplasmic reticulum (ER) function is impaired. Recent studies demonstrated that ER stress can also induce cell-specific genes. In this study, we examined whether X-box binding protein 1 (XBP1), a major UPR-linked transcriptional factor, regulates the expression of brain natriuretic peptide (BNP) in cardiomyocytes. In samples from failing human hearts, extensive splicing of XBP1 was observed along with increased expression of glucose-regulated protein of 78 kDa (GRP78), a target of spliced XBP1 (sXBP1), suggesting that the UPR was induced in heart failure in humans. Interestingly, quantitative real-time PCR revealed a positive correlation between cardiac expression of GRP78 and BNP, leading us to test the hypothesis that sXBP1 regulates BNP as well as GRP78 in cardiomyocytes. A pharmacological ER stressor caused a dose-dependent increase in the expression of sXBP1 and BNP by cultured cardiomyocytes. Short interfering RNA targeting XBP1 suppressed the induction of BNP expression by a pharmacological ER stressor or norepinephrine, which was rescued by the adenovirus-mediated overexpression of sXBP1. The promoter assay with overexpression of sXBP1 or norepinephrine showed that the proximal AP1/CRE-like element in the promoter region of BNP was critical for transcriptional regulation of BNP by sXBP1. Direct binding of sXBP1 to this element was confirmed by the chromatin immunoprecipitation assay. These findings suggest that ER stress observed in failing hearts regulates cardiac BNP expression through a novel promoter region of the AP1/CRE-like element.

1. Introduction

The endoplasmic reticulum (ER) is an organelle that synthesizes and folds both secretory and membrane proteins [1–3]. Stresses that interfere with ER function lead to the accumulation of unfolded and misfolded proteins, after which the ER transmembrane sensors detect their accumulation and initiate the unfolded protein response (UPR) to maintain ER function [1–3]. Recently, we and others have demonstrated the increased expression of genes targeted by the UPR, such as glucose-regulated protein of 78 kDa (GRP78) and protein disulfide isomerase, in patients with cardiovascular disease, suggesting that activation of the UPR is involved in the pathophysiology of such diseases [1,4,5].

The transcriptional factor X-box binding protein 1 (XBP1) is uniquely regulated by inositol requiring kinase 1α (IRE1α), which is an ER stress sensor conserved in all eukaryotic cells [6]. Interestingly, when IRE1α is activated and senses unfolded proteins in the ER, it promotes an increase of endoribonuclease activity that specifically cleaves the mRNA encoding XBP1 (unspliced XBP1) to form transcriptionally active XBP1 (spliced XBP1) [1–3,6]. Spliced XBP1 (sXBP1) binds to ER stress response elements I and II (ERSE-I; CCAAT (N9)CCACG; ERSE-II; ATTGG(N1)CCACG) and mammalian UPR element (mUPRE; TGACGTGG/A) to regulate a variety of UPR target genes that include ER-resident chaperones and genes involved in ER associated protein degradation and lipid biosynthesis [7,8]. In addition to the induction of UPR-related genes by ER stress, recent studies demonstrated that ER stress also induces unexpected genes in

Abbreviations: BNP, brain natriuretic peptide; cDNA, complementary DNA; ER, endoplasmic reticulum; ERSE-I, -II, ER stress response elements I, II; GAPDH, glyceraldehyde-3-phosphate dehydrogenase; GRP78, glucose-regulated protein of 78 kDa; IRE1α, inositol requiring kinase 1α; mUPRE, mammalian UPR element; NE, norepinephrine; RT-PCR, real-time polymerase chain reaction; siRNA, short interfering RNA; sXBP1, spliced X-box binding protein 1; TU, tunicamycin; uXBP1, unspliced X-box binding protein 1; UPR, unfolded protein response.

* Corresponding author. Department of Cardiovascular Medicine, Osaka University Graduate School of Medicine, 2-2 Yamadaoka, Suita, Osaka 565-0871, Japan. Tel.: +81 6 6879 3635; fax: +81 6 6879 3645.
E-mail address: minamino@cardiology.med.osaka-u.ac.jp (T. Minamino).

0022-2828/$ – see front matter © 2010 Elsevier Ltd. All rights reserved.
doi:10.1016/j.yjmcc.2010.02.004

cell type- and condition-specific manner [9,10]. However, the genes altered by the sXBP1 in cardiomyocytes have not been well clarified. In the present study, we found extensive splicing of XBP1 and positive correlation between cardiac expressions of GRP78 and BNP in human normal and failing heart samples. Then we found that sXBP1 regulates BNP expression via a novel region of the BNP promoter in cultured cardiomyocytes. To our knowledge, this is the first information that links the UPR and the natriuretic peptide system which plays an important role in maintenance of the fluid balance and in cardiovascular growth [11].

2. Materials and methods

2.1. Materials

Tunicamycin (TU) and norepinephrine (NE) were purchased from Sigma Chemical Co. (St. Louis, MO, USA). Antibodies for XBP1, α- and β-actin were obtained from Santa Cruz Biotechnology (Santa Cruz, CA, USA). An antibody for HP1α was obtained from Sigma Chemical Co. HS-142-1 was kindly provided by Kirin-Kyowa Pharmaceutical Co. (Tokyo, Japan).

2.2. Human heart tissue samples

Human heart tissue samples were studied according to the protocol approved by the Institutional Review Boards of Hayama Heart Center and Osaka University. We used heart samples of left ventricle from 4 patients with heart failure who underwent partial left ventriculoplasty at Hayama Heart Center. Messenger RNA of 2 control left ventricle heart samples were obtained commercially from Clontech Labs (Mountain View, CA, USA) and Stratagene (La Jolla, CA, USA). Tissue samples were frozen at −80 °C until use for extraction of RNA.

2.3. Analysis of XBP1 mRNA processing

Evaluation of XBP1 mRNA splicing was performed as described previously [12]. In brief, splicing of XBP1 mRNA by activated IRE1 creates a frame shift [6].Complementary DNA (cDNA) was prepared from human heart samples and rat cardiomyocytes. Using this cDNA as a template, PCR was performed with specific primers for XBP1 that covered the splicing site. (Human: sense primer: 5′-CCTTGTAGTTGAGAACCAGG-3′ and anti-sense primer: 5′-GGGGCTTGGTATATATGTGG-3′, rat: sense primer: 5′-ACGAGAGAAAACTCATGG-3′ and anti-sense primer: 5′-ACAGGGTCCAACTTGTCC-3′). The human PCR amplification products were 416 (spliced) and 442 (unspliced) base pairs (bp) in size, respectively. The rat PCR amplification products were 290 (spliced) and 264 (unspliced) base pairs (bp) in size, respectively. The products were separated on 5% polyacrylamide gel, visualized under UV light and quantified by densitometry (Scion Image software).

2.4. Preparation of neonatal rat cardiomyocytes

Primary cultures of cardiomyocytes were prepared from neonatal rat hearts as described previously [13]. All procedures were done in accordance with the guiding principles of Osaka University School of Medicine, the "Position of the American Heart Association on Research Animal Use", and the "Guide for the Care and Use of Laboratory Animals" published by the US National Institute of Health (NIH Publication No. 85-23, revised 1996).

2.5. Immunoblot analysis

Preparation of cardiomyocytes, electrophoresis, immunoblotting, and detection were all done as described previously [13]. Nuclear and cytosolic fractions were separated by Dignam's method [14]. HP1α and beta-actin were used as controls for the nuclear and cytosolic fractions, respectively.

2.6. Quantitative real-time PCR (RT-PCR)

Human or rat samples were prepared according to the Omniscript Reverse Transcription Handbook (QIAGEN Inc.). The primers and probes used for quantification of sXBP1, BNP, GRP78, and GAPDH were all designed according to the manufacturer's protocol (Applied Biosystems, Foster City, CA. https://www.appliedbiosystems.com/). Quantitative RT-PCR was performed as described previously [13].

2.7. RNA interference

We obtained the short interfering RNAs (siRNAs) from B-Bridge International, Inc. to knock-down rat, but not human, XBP1 mRNA (XBP1-1 siRNA: 5′-GAGAAAGCGCUGCGGAGGA-3′, XBP1-2 siRNA: 5′-CUUCAAAGGUAUUCCAAUA-3′) or rat BNP mRNA (BNP siRNA: 5′-CAAACUUGCCACAGUGUAA-3′), as described previously [13]. Bioinformatic analysis reveals that rat siRNA targeting XBP1 did not knock-down human XBP1. Transfection of the siRNAs was performed as described previously [13].

2.8. Adenovirus transduction

Adenoviral vectors containing the genes for LacZ and spliced human XBP1 were prepared as described previously [13]. Adenovirus carrying LacZ or spliced XBP1 was transfected at 24 h after the isolation of cardiomyocytes, and experiments were performed 48 h after transfection.

2.9. Microarray analysis

For microarray analysis, 3 RNA samples of cardiomyocytes transfected with adenovirus carrying LacZ (80 MOI) or spliced XBP1 (80 MOI) for 48 h were used. Cardiac gene expression was determined using GeneChip Rat Genome 230 2.0 Array (Affymetrix). All expression data were normalized by global scaling and analyzed by GeneSpring software (Agilent Technologies).

2.10. Confocal fluorescence microscopy

Cells were plated at a concentration of 1×10^6 cells/plate and viewed with confocal fluorescence microscopy (Radiance 2100 Laser Scanning System, Bio-Rad, Heimei Hempstead, UK), as described previously [13]. Cell surface area was measured using ImageJ (http://rsb.info.nih.gov/ij/) from 30 randomly selected cells per experiment.

2.11. Assessment of cardiomyocyte viability

The viability of cardiomyocytes was evaluated as described previously [13]. The dose of HS-142-1 used in the present study efficiently blocked BNP receptor [15].

2.12. Plasmid construction

Progressive deletion fragments of the 5′ flanking region of the BNP gene were amplified by PCR with sense primers containing an additional Kpn1 site (hBNP-1780F: 5′-GGTACCCCCTGGCAGTGATTATGAGCTTCA-3′, hBNP-238F; 5′-GGTACCGGGACTTGTCTGTGTCTCCA-3′, hBNP-111F; 5′-GGTACCTGATCTCAGAGGCCCGGAATGT-3′, hBNP-101F; 5′-GGTACCGGCCCGGAATGTGGCTGATAAAT-3′) and an antisense primer containing a Hind III site (hBNP + 61R; 5′-AAGCTTGCTGCTGCTGCGATGCGTCCGGGTTTGCTT-3′). After digestion with Kpn1 and Hind III, the fragments were inserted between the Kpn1 and Hind

III sites in the firefly luciferase reporter plasmid pGL3-Basic (Promega). A deletion mutant lacking the AP1/CRE-like element was amplified by PCR with a sense primer (hBNP-103F: 5′-GAGGCCCGGAATGTGGCTGATAAAT-3′) and an anti-sense primer (hBNP-112R: 5′-GGGCCCGGGAATGAGCCCCTCCGCGCCT-3′), and was inserted into the pGL3-Basic plasmid. The plasmid for human sXBP1 was a kind gift from Dr. K. Mori (Kyoto University, Japan).

2.13. Luciferase gene reporter assay

Freshly prepared rat cardiomyocytes (4×10^6 cells) were transiently co-transfected with 10 μg of the indicated reporter construct and 10 μg of control vector (Renilla luciferase plasmid pRL-SV40) with or without 10 μg of the effector plasmid carrying sXBP1 cDNA. Electroporation was done at 280 V/300 μF in 0.2-cm cuvettes. Then the cells were plated into fibronectin-coated six-well culture dishes and incubated for 72 h to allow attachment. For the NE experiment, cardiomyocytes were co-transfected with the indicated reporter construct and control vector and maintained for 48 h. Then, they were treated with NE (1 μmol/L) for 24 h. Subsequently, luciferase activity of cell lysates was measured with a luminometer according to the manufacturer's protocol (Dual-Luciferase Reporter Assay; Promega), and reporter activity was calculated as the relative luciferase activity (firefly luciferase/Renilla luciferase) to correct for variations in transfection efficiency.

2.14. Chromatin immunoprecipitation (ChIP) assay

Rat neonatal cardiomyocytes (5×10^6) were transfected with adenovirus carrying human sXBP1 or LacZ and incubated for 48 h before being cross-linked with 1% formaldehyde. The ChIP assay was performed using a Chromatin Immunoprecipitation Assay Kit (Upstate) according to the manufacturer's protocol. The P1/P2 primers used for detection of rat BNP were 5′-GACAACACCAGCTGCAGGATGGGCTTGACGGCAAGT-3′ (rBNP-2863F) and 5′-CCGACCTCTGTGCATCAATGGTA-3′ (rBNP-2706R), yielding a 157 bp product. The P3/P4 primers used for detection of rat BNP were 5-GGAAACAAGGACCTGTTAGTGT-3′ (rBNP-257F) and 5-GGGTGGGGTTATCTCTGATTT-3′ (rBNP-72R), yielding a 185 bp product.

2.15. Statistical analysis

Data are expressed as the mean ± S.E.M. Unpaired Student *t*-test was used to compare the expression of BNP and GRP78 in human hearts. Spearman rank correlation analysis was used to examine the relationship between cardiac mRNA levels of targeted genes. The results of quantitative RT-PCR, cardiomyocyte viability analysis, and the promoter assay were compared by one-way factorial ANOVA followed by Bonferroni's correction. Microarray data was analyzed using unpaired *t*-test. For all analyses, $P<0.05$ was accepted as statistically significant.

3. Results

3.1. Extensive XBP1 splicing and increased expression of GRP78 and BNP in human failing hearts

To investigate activation of the UPR in failing human hearts, we determined the extent of XBP1 mRNA splicing as an indicator of UPR activation in samples of normal and failing myocardium. The clinical characteristics of patients were listed in the Table 1. The major form of XBP1 in normal human hearts was unspliced, while the major form in failing hearts was spliced (Fig. 1A). Consistent with these findings about XBP1 activation, quantitative RT-PCR revealed that expression of GRP78, a target of sXBP1, was significantly higher in failing hearts ($n=4$) than in normal hearts ($n=2$) (Fig. 1B). These findings suggest that the UPR was activated in failing human hearts. In addition, the BNP mRNA level was significantly higher in failing human hearts ($n=4$) compared with that in normal hearts ($n=2$) (Fig. 1C). Importantly, the quantitative real-time PCR revealed a positive correlation between cardiac expressions of GRP and BNP (Fig. 1D). There was no significant correlation between sXBP1 and GRP78 (Fig. 1E) or BNP (Fig. 1F).

Table 1
Clinical characteristics of patients.

Age	Gender	Diagnosis	BNP (pg/mL)	NYHA class	Echocardiographic findings		
					EF (%)	LVDd (mm)	LVDs (mm)
69	M	DCM	465	III	30	86	73
63	M	DCM	621	III	28	68	58
59	M	ICM	104	III	18	71	58
57	M	ICM	166	III	15	77	68

DCM, dilated cardiomyopathy; ICM, ischemic cardiomyopathy; BNP, brain-type natriuretic peptide; NYHA, New York Heart Association function class; LVEF, left ventricular ejection fraction; LVDd, left ventricular end-diastolic dimension; LVDs, left ventricular end-systolic dimension.

3.2. A pharmacological ER stressor increases BNP expression via an XBP1-dependent pathway in rat neonatal cardiomyocytes

Then, we investigated whether ER stress could induce BNP expression via an XBP1 dependent pathway. PCR analysis showed that treatment of cardiomyocytes with tunicamycin (TU), a pharmacological ER stressor, increased the level of mRNA for spliced XBP1 (Fig. 2A). TU increased the protein levels of nuclear, but not cytosolic, XBP1 protein (Fig. 2A) and mRNA levels of BNP (Fig. 2B) in rat cardiomyocytes. When we transfected a different dose of siRNA targeting XBP1 (siRNA-XBP1-1), siRNA targeting XBP1 dose-dependently reduced protein levels of nuclear XBP1 and mRNA levels of BNP by tunicamycin (Fig. 2C). When we transfected 2 different siRNAs targeting XBP1, either of the siRNAs targeting XBP1 efficiently reduced XBP1 protein levels (Fig. 2D). We also found that increased expression of BNP in response to pharmacological ER stress was significantly attenuated by 2 different siRNAs targeting XBP1 (Fig. 2E). These findings suggested that pharmacological ER stress induces BNP expression via an XBP1-dependent pathway in cultured rat cardiomyocytes.

3.3. Adenovirus-mediated overexpression of spliced XBP1 increases BNP expression in cultured rat cardiomyocytes

Next, we investigated the influence of sXBP1 on BNP expression by cultured rat cardiomyocytes. Immunohistological analysis revealed the nuclear localization of XBP1 in rat cardiomyocytes infected with adenovirus carrying sXBP1, but not LacZ (Fig. 3A). The transfection of adenovirus carrying sXBP1 or LacZ did not change the cardiomyocyte size (Fig. 3B). An increase of nuclear XBP1 protein levels by the overexpression of sXBP1 was also confirmed by immunoblot analysis (Fig. 3C). Adenovirus-mediated overexpression of sXBP1 increased mRNA levels of GRP78 (Fig. 3D) and BNP (Fig. 3E) in a dose-dependent manner.

Since the stimuli that enhance BNP expression often activate hypertrophic program, we checked the expression levels of representative hypertrophic genes when cardiomyocytes were transfected with adenovirus carrying LacZ ($n=3$) or sXBP1 ($n=3$): BNP (0.47 ± 0.07 versus 1.47 ± 0.04, $P=0.0002$), GRP78 (0.83 ± 0.12 versus 1.81 ± 0.25, $P=0.02$), β-myosin heavy chain (MHC) (0.93 ± 0.05 versus 1.05 ± 0.04, $P=0.15$), atrial natriuretic peptide (ANP) (0.86 ± 0.08 versus 1.10 ± 0.04, $P=0.06$), α-actin (0.35 ± 0.13 versus 1.46 ± 0.03, $P=0.001$), α-MHC (1.00 ± 0.00 versus 0.73 ± 0.14, $P=0.12$) and sarcoendoplasmic reticulum Ca ATPase (SERCA) (0.96 ± 0.04 versus 0.97 ± 0.19, $P=0.95$). These findings suggest that hypertrophic genes

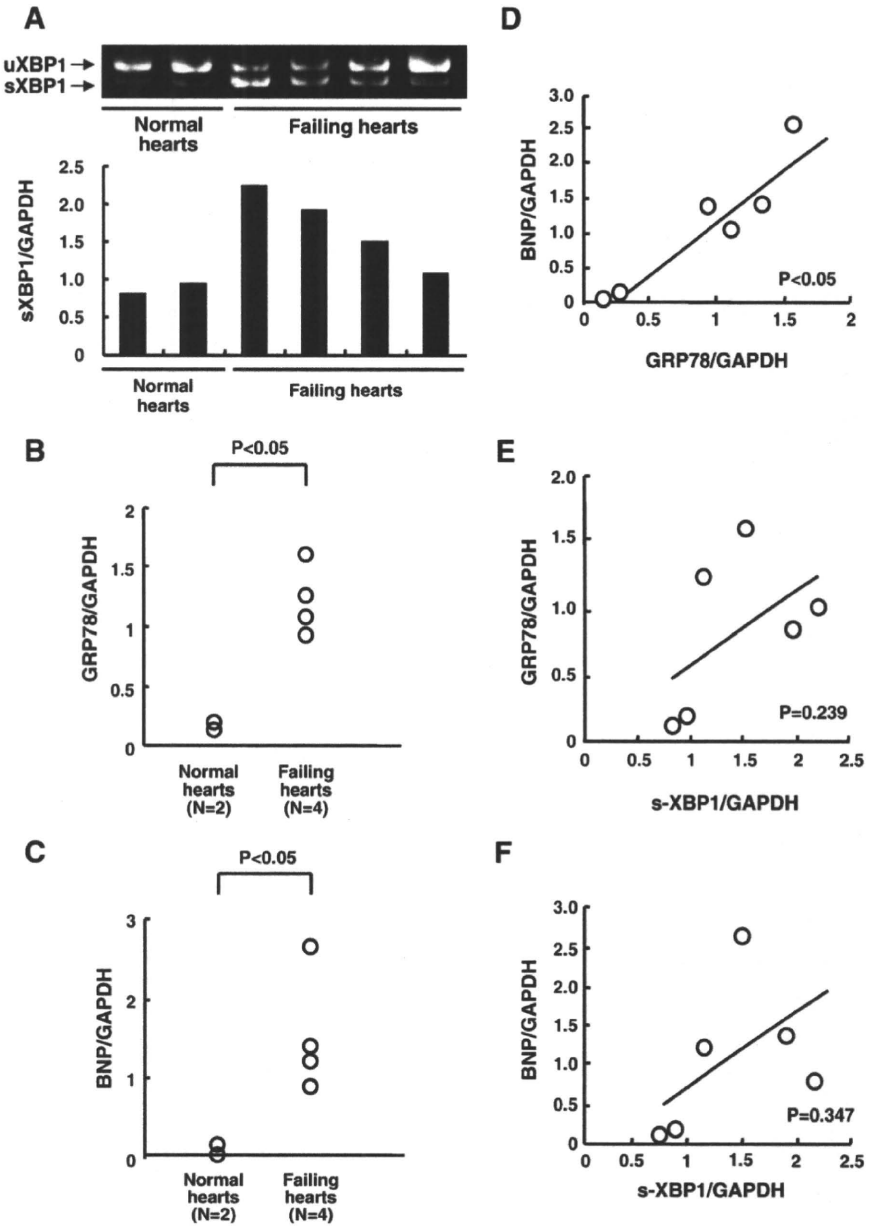

Fig. 1. UPR signaling in human hearts. (A) (Upper panel) Splicing of XBP1 mRNA in myocardial tissue from normal ($n=2$) and failing ($n=4$) human hearts. (Lower panel) Quantitative analysis of sXBP1 in normal and failing human hearts. uXBP1 and sXBP1 indicate unspliced and spliced XBP1, respectively. (B, C) Quantitative analysis of GRP78 (B) and BNP (C) mRNA in normal and failing human hearts. (D) Relationship between the cardiac expression of GRP78 and BNP in normal and failing human hearts. (E, F) Relationship between the cardiac expression of sXBP1 and GRP78 (E) or BNP (F) in normal and failing human hearts. All results of quantitative RT-PCR were normalized for GAPDH expression.

except α-actin did not significantly alter by the overexpression of sXBP1. Furthermore, overexpression of sXBP1 did not alter cardiomyocyte viability, suggesting that sXBP1 did not induce BNP secondary to cellular damage (data not shown). Importantly, we found that overexpression of sXBP1, but not LacZ, could rescue the tunicamycin-mediated enhancement of BNP that was blocked by siRNA for XBP1 (Fig. 3F). We could not detect the binding of XBP1 to the proximal AP1/CRE-like element in the BNP promoter in response to a pharmacological stressor (data not shown).

3.4. Spliced XBP1 binds to an AP1/CRE-like element in the BNP promoter region and increases its promoter activity

To investigate whether or not sXBP1 activated the transcription of BNP, we performed a number of luciferase reporter assays, in which cultured cardiomyocytes were co-transfected with a series of reporter plasmids containing fragments of the BNP 5′-flanking region (from −1780 to −101) and the pGL3 vector with or without sXBP1. Under baseline conditions, transfection of longer reporter plasmids containing the promoter region (−238 to −111) increased luciferase activity compared with transfection of the reporter plasmid lacking the promoter region (−238 to −111) or the empty pGL3-Basic plasmid (Fig. 4A left). These findings suggested that the proximal region (−238 to −111) was essential for BNP promoter activity under baseline conditions. After transfection of the pGL3-Basic vector containing spliced XBP1 (inducible conditions), co-transfection of the reporter gene containing the region (−111 to −101) increased luciferase activity by 3- to 4-fold compared with the control (empty pGL3-Basic vector) or the reporter gene lacking this region (Fig. 4A right). The bioinformatic analysis revealed that the BNP promoter

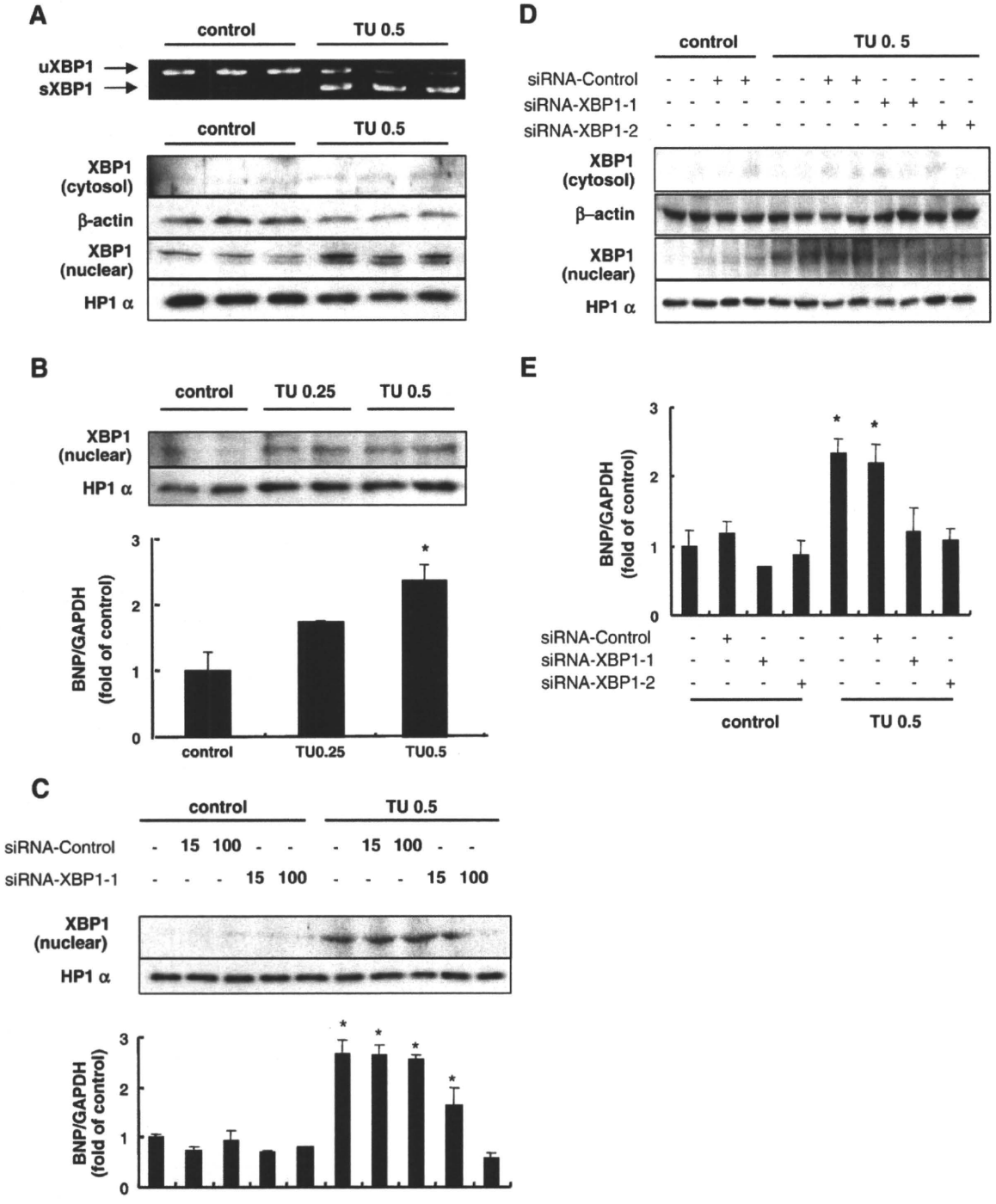

Fig. 2. A pharmacological ER stressor increases BNP expression via an XBP1-dependent pathway in rat neonatal cardiomyocytes. (A) Effects of TU on splicing of XBP1 in cultured cardiomyocytes. Neonatal rat cardiomyocytes were maintained for 24 h and then treated with TU (0.5 μg/mL) for the next 24 h. Evaluation of XBP1 splicing was performed by quantitative RT-PCR (upper panel) and immunoblot analysis (lower panel). (B) Dose-dependent effects of TU (0.25 or 0.5 μg/mL) on protein levels of XBP1 in the nuclear fraction (upper panel) and mRNA levels of BNP (lower panels) in cultured cardiomyocytes. HP1α was used as the internal control for protein levels in nuclear fraction. Results were expressed as the mean ± SEM. *$P<0.05$ versus control. (C) Dose–response effects of siRNA for XBP1 on BNP expression. Neonatal rat cardiomyocytes were maintained for 6 h and then were treated with different dose of control and XBP1 siRNA (15 μmol/L and 100 μmol/L) for 18 h. Subsequently, cardiomyocytes were treated with TU (0.5 μg/mL) for 24 h. (D, E) Effects of 2 different siRNAs targeting XBP1 on the protein level of XBP1 (D) and mRNA level of BNP (E) in cardiomyocytes treated with TU. Experiments were repeated twice independently ($n=2$–3 per experiment). Results are expressed as the mean ± SEM. *$P<0.05$ versus control.

region (−111 to −101) corresponded to an AP1/CRE-like element, which is well conserved among mammals (Fig. 4B). These findings suggested that the AP1/CRE-like element is essential for BNP promoter activity under inducible conditions.

Next, we transfected reporter plasmids containing the BNP promoter region (−1780 to +63) with and without the AP1/CRE-like element (−111 to −101). Deletion of the AP1/CRE-like element resulted in a significant decrease of luciferase activity under inducible

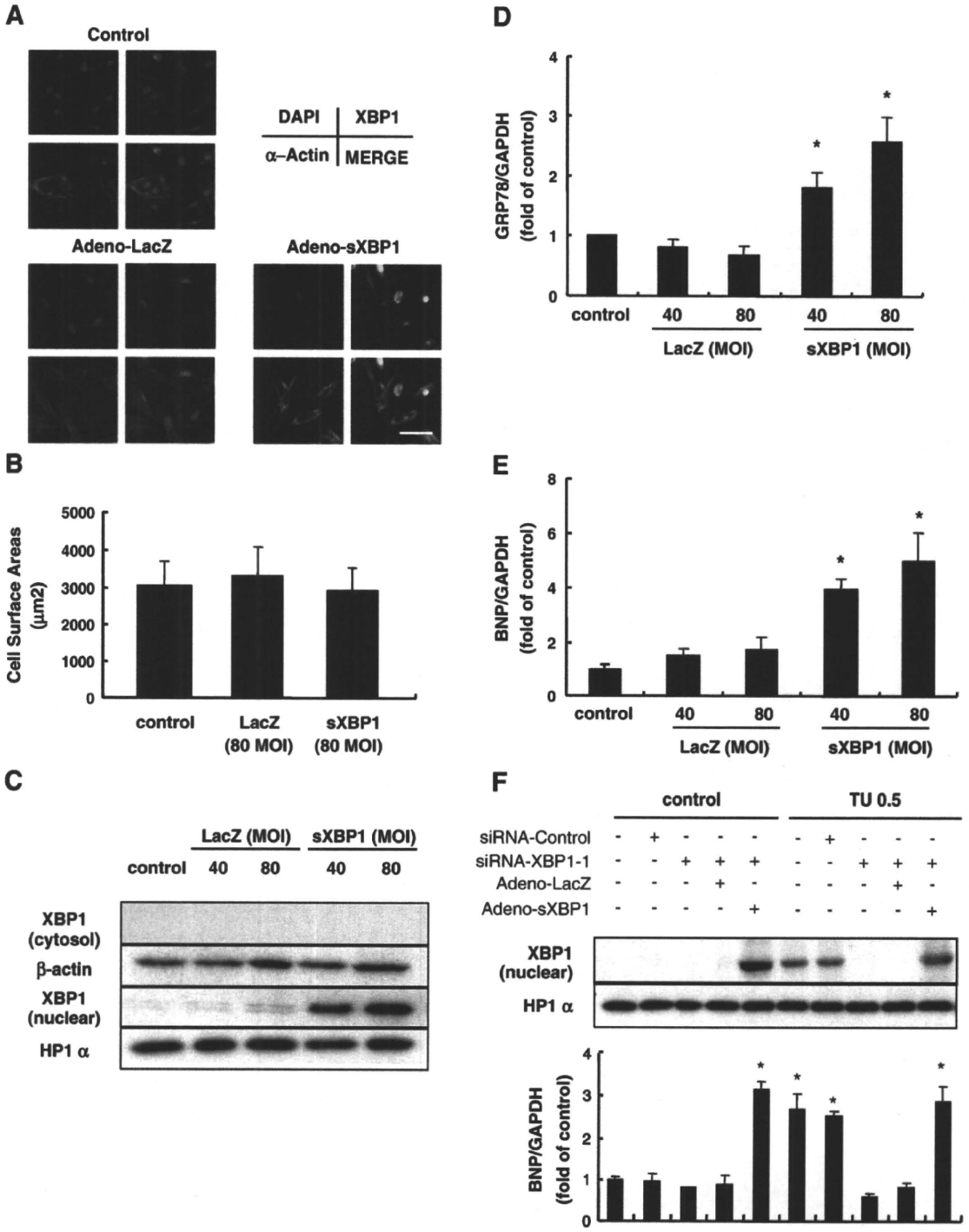

Fig. 3. Adenovirus-mediated overexpression of spliced XBP1 increases BNP expression in neonatal rat cardiomyocytes. (A) Representative immunohistochemistry of XBP1 expression in cultured rat cardiomyocytes. Confocal fluorescence microscopy shows XBP1, α-actin, and DAPI by green, red and blue staining, respectively. Bar indicates 20 μm. (B) Effects of adenovirus-mediated overexpression of LacZ or spliced XBP1 on cardiomyocyte size. (C) Immunoblot analysis of XBP1 in the nuclear and cytosolic fractions. HP1α and β-actin were used as the internal controls for the nuclear and cytosolic fractions, respectively. XBP1 in cytosolic fractions was not observed due to the rapid degradation by proteasome. Effects of overexpression of spliced XBP1 on GRP78 (D) and BNP (E) mRNA levels in cultured cardiomyocytes. MOI indicates multiplicity of infection. (F) Effects of overexpression of XBP1 on mRNA level of BNP that is blocked by siRNA for XBP1. Cardiomyocytes were treated with siRNA targeting XBP1 for 24 h and were treated with tunicamycin (0.5 μg/mL) for the next 24 h. Thereafter, they were incubated with an adenoviral vector carrying LacZ (80 MOI) or spliced XBP1 (80 MOI) for 48 h. Experiments were repeated twice independently ($n = 2$–3 per experiment). Results were expressed as the mean ± SEM. *$P<0.05$ versus control.

conditions by overexpression of sXBP1 (Fig. 4C), but not baseline ones.

We also examined the role of XBP1 in BNP expression in response to NE. We found that the NE (1 μmol/L) for 24 h increased protein levels of XBP1 in the nuclear fractions and BNP expression in cultured cardiomyocytes, which was significantly attenuated by siRNA targeting XBP1. The quantitative real-time analysis revealed that the siRNA targeting sXBP1 did not block the enhancement of ANP by NE

(Control: 1.00 ± 0.16; NE: 1.61 ± 0.19; NE + siRNA XBP1: 1.67 ± 0.31; $n = 3$ in each group), suggesting that XBP1 is not involved in hypertrophic program in response to NE. These findings suggest that XBP1 is involved in BNP expression in response to NE as well as a pharmacological ER stressor. Deletion of the proximal AP1/CRE-like element resulted in a significant decrease of luciferase activity in response to NE (Fig. 4D).

Finally, we performed the ChIP assay to determine whether sXBP1 binds to the AP1/CRE-like element of the endogenous BNP promoter in vivo. Chromatin from cardiomyocytes transfected with adenovirus carrying LacZ or sXBP1 was immunoprecipitated with an antibody directed against XBP1. PCR products were obtained by using primers that covered the AP1/CRE-like element (P3/P4), but not with primers covering the −2863 to −2706 region (P1/P2) (Fig. 4E).

3.5. Induction of BNP by pharmacological ER stress does not affect the viability of cultured cardiomyocytes

We investigated the effect of the induction of BNP by pharmacological ER stress on cell viability. The siRNA targeting BNP reduced the BNP mRNA level by 93% ($n = 4$). There was no difference of cell viability when cardiomyocytes were treated with the siRNA targeting BNP (Fig. 5A) or a BNP receptor antagonist (HS-142-1) followed by a pharmacological ER stressor (Fig. 5B). These findings suggested that the induction of BNP by ER stress did not directly prevent cardiac cell death by ER stress.

4. Discussion

4.1. The UPR in heart failure

The ER is an organelle with a role in protein folding, calcium homeostasis, and lipid biosynthesis. Failing hearts show oxidative stress, hypoxia, and enhanced protein synthesis, any of which could potentially lead to ER dysfunction [1–3]. Indeed, we and others have found extensive splicing of XBP1 and increased expression of GRP78 in failing human hearts, suggesting that the UPR is activated in diseased hearts [6,7,16]. Consistent with previous reports, we also found an increase of BNP mRNA levels in myocardial samples from failing human hearts, which is widely used as a marker of heart failure [11,17]. Although the UPR triggers signaling that induces genes to maintain ER function, recent studies have shown that the UPR is also linked to other physiological systems [9,10]. Interestingly, we found a positive correlation between cardiac expression of GRP78 and BNP in human samples. These findings led us to hypothesize that BNP as well as GRP78 are commonly regulated by an UPR-dependent mechanism, although BNP has not previously been recognized as one of the targets of the UPR. Disappointingly, cardiac expressions of sXBP1 did not correlate with those of GRP78 or BNP probably due to the multiple factors that would modify their cardiac expressions in the clinical settings.

4.2. BNP expression is regulated by XBP1 in cardiomyocytes

To investigate whether BNP expression was regulated by ER stress, we treated cultured cardiomyocytes with a pharmacological ER stressor, tunicamycin, which is an inhibitor of glycosylation. This agent dose-dependently increased the expression of BNP in cultured cardiomyocytes, suggesting that BNP expression is upregulated in response to ER stress. We also confirmed that sXBP1 had a crucial role in the cardiac expression of BNP as well as GRP78 in response to a pharmacological ER stressor by experiments using 2 different siRNAs against XBP1 or an adenovirus vector carrying sXBP1. Since we showed that overexpression of sXBP1 increased BNP expression without affecting cardiomyocyte viability, the elevation of BNP expression did not seem to be due to cellular damage caused by adenoviral transfection.

Many hypertrophic stimuli can enhance BNP expression along with both the activation of hypertrophic program and the increase in cardiomyocytes size [18]. Thus, we performed microarray analysis to check whether overexpression of sXBP1 could alter the representative hypertrophic gene expressions. We found that these genes except α-actin did not significantly alter by the overexpression of sXBP1. Interestingly, bioinformatic analysis reveals that there exists AP1/CRE-like element in the promoter region of α-actin (−520 to −513). These results would strength the findings that sXBP1 could regulate the expression of some genes through the AP1/CRE-like element. Furthermore, the overexpression of sXBP1 did not change the size of cultured cardiomyocytes and the siRNA for sXBP1 did not block the enhancement of ANP by NE. These findings also suggest that sXBP1 enhances BNP expression without altering hypertrophic program.

In addition to sXBP1, several factors are involved in the transcription of genes targeted by the UPR [1–3]. These UPR-linked transcriptional factors independently, and sometimes cooperatively, regulate the target genes in response to ER stress [1–3]. Since 2 different siRNAs targeting XBP1 almost completely suppressed BNP expression by tunicamycin and overexpression of sXBP1 could rescue the tunicamycin-mediated enhancement of BNP that was blocked by siRNA targeting XBP1, sXBP1 seems to be an essential regulator of BNP transcription in response to ER stress.

4.3. Spliced XBP1 binds to the BNP promoter response element and increases its promoter activity

Spliced XBP1 is known to bind to certain promoter regions, including ERSE-I, ERSE-II, and mUPRE [7,8], but our bioinformatics analysis revealed that the promoter region of BNP does not include any of these regions. Surprisingly, the promoter assay revealed that the AP1/CRE-like element (−111 to −103) of the BNP promoter was essential for its enhanced activity by spliced XBP1. The ChIP assay also demonstrated that spliced XBP1 bound to the AP1/CRE-like element. AP-1/CRE-like element is the site overlapped by AP-1 and CRE binding sequence [19,20]. Although several factors are reported to bind to this element, to our knowledge, this is the first to show that sXBP1 can bind to this region. Bioinformatic analysis revealed that BNP promoter has 3 different AP-1/CRE-like elements (TGATCTCA at −111; TGAGATCA at −385; and TGACATCA at −1472). Importantly, the promoter assay analysis demonstrated that the only proximal AP-1/CRE-like element has the function to enhance BNP expression in response to spliced XBP-1. Lapointe et al. demonstrated that the proximal AP1/CRE-like element (−111 to −103) is required for BNP expression in response to mitogen activated protein kinase (MAPK) kinase 6 or p38 MAPK [21]. Consistently, another study also demonstrated that only one specific element can play an important role in gene regulation although several of the same elements exist in the promoter region [22].

Although we performed ChIP assay using a pharmacological ER stressor, we could not detect the binding of XBP1 to the proximal AP1/CRE-like element in the BNP promoter (data not shown). One possible explanation for this failure would be due to the difference in sXBP1 levels in experiments using XBP1 overexpression and pharmacological treatment. Furthermore, we tried to use 2 different antibodies against XBP1 for the ChIP assay, but we could detect the binding only when we used the antibody presented in the manuscript. Thus, the technical limitation would be the possible explanation for the failure to detect the binding using a pharmacological ER stressor.

Recent studies demonstrated that NE can induce ER stress in PC12 cells [23,24]. The present study revealed that NE increased protein levels of sXBP1 and that BNP expression in response to NE was blocked by siRNA against XBP1. Since adrenergic systems are activated in patients with heart failure, increased levels of NE might regulate BNP via ER stress related pathways. Since NE can activate both MAPK- and XBP1-dependnt pathways, further investigation will be required for the interaction between sXBP1 and MAPK in the BNP expression through the proximal Ap1/CRE-like element [20,21].

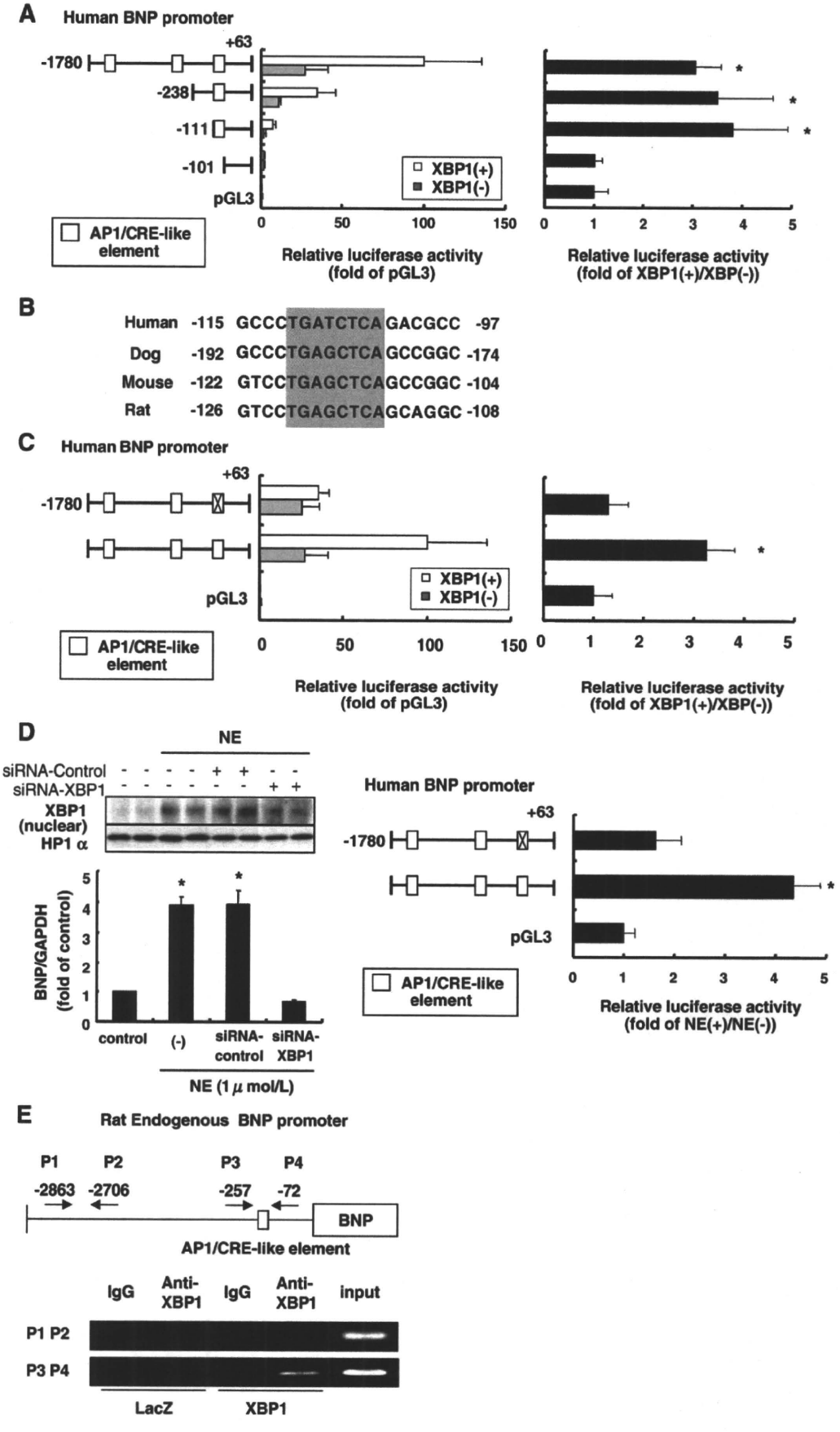
A
Human BNP promoter
+63
-1780
-238
-111
-101
pGL3
XBP1(+)
XBP1(-)
AP1/CRE-like element
0 50 100 150
Relative luciferase activity (fold of pGL3)
0 1 2 3 4 5
Relative luciferase activity (fold of XBP1(+)/XBP(-))
B
Human -115 GCCCTGATCTCAGACGCC -97
Dog -192 GCCCTGAGCTCAGCCGGC -174
Mouse -122 GTCCTGAGCTCAGCCGGC -104
Rat -126 GTCCTGAGCTCAGCAGGC -108
C
Human BNP promoter
+63
-1780
pGL3
XBP1(+)
XBP1(-)
AP1/CRE-like element
0 50 100 150
Relative luciferase activity (fold of pGL3)
0 1 2 3 4 5
Relative luciferase activity (fold of XBP1(+)/XBP(-))
D
NE
siRNA-Control - - - - + + - -
siRNA-XBP1 - - - - - - + +
XBP1 (nuclear)
HP1 α
BNP/GAPDH (fold of control)
0 1 2 3 4 5
control
(-)
siRNA-control
siRNA-XBP1
NE (1 μ mol/L)
Human BNP promoter
+63
-1780
pGL3
AP1/CRE-like element
0 1 2 3 4 5
Relative luciferase activity (fold of NE(+)/NE(-))
E
Rat Endogenous BNP promoter
P1 P2 P3 P4
-2863 -2706 -257 -72
BNP
AP1/CRE-like element
IgG Anti-XBP1 IgG Anti-XBP1 input
P1 P2
P3 P4
LacZ
XBP1

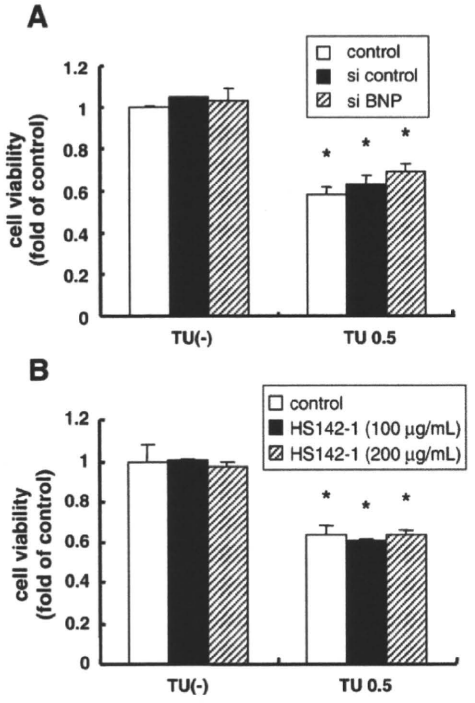

Fig. 5. Induction of BNP by pharmacological ER stress does not affect the viability of cultured cardiomyocytes. Effect of siRNA targeting BNP or HS-142-1, a BNP receptor blocker, on cardiomyocyte death after exposure to pharmacological ER stress with TU. (A) Neonatal rat cardiomyocytes were maintained for 6 h and then treated with BNP siRNA for 18 h. Subsequently, cardiomyocytes were treated with TU (0.5 μg/mL) for 24 h and cell viability was evaluated. (B) Effect of HS-142-1, a BNP receptor blocker, on cardiomyocyte viability after treatment with TU. Neonatal rat cardiomyocytes were maintained for 24 h and then treated with HS-142-1 (100 or 200 μg/mL) for 6 h. Subsequently, the cells were treated with TU (0.5 μg/mL) for 24 h and their viability was evaluated. Three independent experiments were done to assess cell viability ($n=6$ per experiment). *$P<0.05$ versus no treatment.

4.4. Pathophysiological role of BNP induced by XBP1

Since XBP1 mainly regulates UPR-related genes that potentially reduce cell damage due to ER stress, we checked whether the knock-down of BNP mRNA or blockade of the BNP receptor directly influenced cardiac cell viability in response to a pharmacological ER stressor. Our data showed that BNP in response to ER stress did not directly influence cell viability due to ER stress in cardiomyocytes. However, since BNP has an important role in the maintenance of fluid balance and in cardiovascular growth [11], induced BNP by sXBP1 would indirectly contribute to the improvement in cardiac dysfunction in which UPR is activated.

4.5. Conclusion

In the present study, we showed that sXBP1 regulates BNP expression in cultured cardiomyocytes. Regulation of BNP by XBP1 is another intriguing example of integration of the UPR with a range of physiological systems. Furthermore, since BNP is used for the treatment of heart failure [25], drugs targeting spliced XBP1 or the other factors that bind to the AP1/CRE-like element of BNP promoter region could be promising new therapies for heart failure.

Acknowledgments

We thank Dr. Kazutoshi Mori for the generous gift of sXBP1 cDNA and Ms. Akiko Ogai and Mieko Hayakawa for help with the preparation of mRNAs and cardiomyocytes.

This research was supported by grants-in-aid from the Ministry of Health, Labor, and Welfare—Japan; grants-in-aid from the Ministry of Education, Culture, Sports, Science, and Technology—Japan; grants from the Japan Heart Foundation.

References

[1] Minamino T, Kitakaze M. ER stress in cardiovascular disease. J Mol Cell Cardiol Nov 12 2009 Electronic publication ahead of print.
[2] Kaufman RJ. Orchestrating the unfolded protein response in health and disease. J Clin Invest 2002;110:1389–98.
[3] Ron D, Walter P. Signal integration in the endoplasmic reticulum unfolded protein response. Nat Rev Mol Cell Biol 2007;8:519–29.
[4] Okada K, Minamino T, Tsukamoto Y, Liao Y, Tsukamoto O, Takashima S, et al. Prolonged endoplasmic reticulum stress in hypertrophic and failing heart after aortic constriction: possible contribution of endoplasmic reticulum stress to cardiac myocyte apoptosis. Circulation 2004;110:705–12.
[5] Severino A, Campioni M, Straino S, Salloum FN, Schmidt N, Herbrand U, et al. Identification of protein disulfide isomerase as a cardiomyocyte survival factor in ischemic cardiomyopathy. J Am Coll Cardiol 2007;50:1029–37.
[6] Calfon M, Zeng H, Urano F, Till JH, Hubbard SR, Harding HP, et al. IRE1 couples endoplasmic reticulum load to secretory capacity by processing the XBP-1 mRNA. Nature 2002;415:92–6.
[7] Yamamoto K, Yoshida H, Kokame K, Kaufman RJ, Mori K. Differential contributions of ATF6 and XBP1 to the activation of endoplasmic reticulum stress-responsive cis-acting elements ERSE, UPRE and ERSE-II. J Biochem 2004;136:343–50.
[8] Lee AH, Iwakoshi NN, Glimcher LH. XBP-1 regulates a subset of endoplasmic reticulum resident chaperone genes in the unfolded protein response. Mol Cell Biol 2003;23:7448–59.
[9] Acosta-Alvear D, Zhou Y, Blais A, Tsikitis M, Lents NH, Arias C, et al. XBP1 controls diverse cell type- and condition-specific transcriptional regulatory networks. Mol Cell 2007;27:53–66.
[10] Kaser A, Lee AH, Franke A, Glickman JN, Zeissig S, Tilg H, et al. XBP1 links ER stress to intestinal inflammation and confers genetic risk for human inflammatory bowel disease. Cell 2008;134:743–56.
[11] Nishikimi T, Maeda N, Matsuoka H. The role of natriuretic peptides in cardioprotection. Cardiovasc Res 2006;69:318–28.
[12] Back SH, Lee K, Vink E, Kaufman RJ. Cytoplasmic IRE1alpha-mediated XBP1 mRNA splicing in the absence of nuclear processing and endoplasmic reticulum stress. J Biol Chem 2006;281:18691–706.
[13] Fu HY, Minamino T, Tsukamoto O, Sawada T, Asai M, Kato H, et al. Overexpression of endoplasmic reticulum-resident chaperone attenuates cardiomyocyte death induced by proteasome inhibition. Cardiovasc Res 2008;79:600–10.
[14] Dignam JD, Lebovitz RM, Roeder RG. Accurate transcription initiation by RNA polymerase II in a soluble extract from isolated mammalian nuclei. Nucleic Acids Res 1983;11:1475–89.
[15] Horio T, Nishikimi T, Yoshihara F, Matsuo H, Takishita S, Kangawa K. Inhibitory regulation of hypertrophy by endogenous atrial natriuretic peptide in cultured cardiac myocytes. Hypertension 2000;35:19–24.
[16] Dally S, Monceau V, Corvazier E, Bredoux R, Raies A, Bobe R, et al. Compartmentalized expression of three novel sarco/endoplasmic reticulum Ca2+ATPase 3 isoforms including the switch to ER stress, SERCA3f, in non-failing and failing human heart. Cell Calcium 2009;45:144–54.
[17] Woodard GE, Rosado JA. Recent advances in natriuretic peptide research. J Cell Mol Med 2007;11:1263–71.
[18] Akazawa H, Komuro I. Roles of cardiac transcription factors in cardiac hypertrophy. Circ Res 2003 May 30;92(10):1079–88.
[19] Newell CL, Deisseroth AB, Lopez-Berestein G. Interaction of nuclear proteins with an AP-1/CRE-like promoter sequence in the human TNF-alpha gene. J Leukoc Biol 1994;56:27–35.
[20] Barabitskaja O, Foulke Jr JS, Pati S, Bodor J, Reitz Jr MS. Suppression of MIP-1beta transcription in human T cells is regulated by inducible cAMP early repressor (ICER). J Leukoc Biol 2006;79:378–87.
[21] LaPointe MC. Molecular regulation of the brain natriuretic peptide gene. Peptides 2005;26:944–56.

Fig. 4. Spliced XBP1 binds to an AP1/CRE-like element in the BNP promoter region and increases its promoter activity. (A) Mapping of the XBP1-response element in the BNP promoter. Luciferase activity from 3 independent experiments was normalized to Renilla luciferase activity before being compared with the control (pGL3) with and without co-transfection of spliced XBP1. Relative luciferase activity was determined as the average of duplicate measurements in 3 independent experiments. *$P<0.05$ versus control (pGL3). (B) Comparative analysis of the sequence of the AP1/CRE-like element in the BNP promoter. (C, D) Effects of deletion of the AP-1/CRE-like region on BNP promoter activity stimulated by spliced XBP1 or NE (1 μmol/L). The pGL3-BNP-luciferase reporter (−1780/+63) with or without the AP-1/CRE-like element was transfected as described in (A). Experiments were repeated twice independently ($n=2$ per experiment). Relative luciferase activity was determined by averaging duplicate measurements in the 3 independent experiments. *$P<0.05$ versus control (pGL3). (E) Binding of spliced XBP1 to the AP1/CRE-like element in the BNP promoter was demonstrated by the ChIP assay. Chromatin was immunoprecipitated with IgG or an antibody for XBP1. Purified precipitates were analyzed by PCR using primers specific for the AP1/CRE-like element (P3/P4) or the region 3 kb upstream of the BNP promoter (P1/P2).

[22] Yoshida H, Haze K, Yanagi H, Yura T, Mori K. Identification of the cis-acting endoplasmic reticulum stress response element responsible for transcriptional induction of mammalian glucose-regulated proteins. Involvement of basic leucine zipper transcription factors. J Biol Chem 1998 Dec 11;273(50):33741–9.
[23] Mao W, Iwai C, Qin F, Liang CS. Norepinephrine induces endoplasmic reticulum stress and downregulation of norepinephrine transporter density in PC12 cells via oxidative stress. Am J Physiol Heart Circ Physiol 2005;288:H2381–9.
[24] Mao W, Iwai C, Keng P, Vulapalli R, Liang CS. Norepinephrine-induced oxidative stress causes PC-12 cell apoptosis by both endoplasmic reticulum stress and mitochondrial intrinsic pathway: inhibition of phosphatidylinositol 3-kinase survival pathway. Am J Physiol Cell Physiol 2006;290:C1373–84.
[25] Colucci WS, Elkayam U, Horton DP, Abraham WT, Bourge RC, Johnson AD, et al. Intravenous nesiritide, a natriuretic peptide, in the treatment of decompensated congestive heart failure. Nesiritide Study Group. N Engl J Med 2000;343:246–53.

Promotion of CHIP-Mediated p53 Degradation Protects the Heart From Ischemic Injury

Atsuhiko T. Naito, Sho Okada, Tohru Minamino, Koji Iwanaga, Mei-Lan Liu, Tomokazu Sumida, Seitaro Nomura, Naruhiko Sahara, Tatsuya Mizoroki, Akihiko Takashima, Hiroshi Akazawa, Toshio Nagai, Ichiro Shiojima, Issei Komuro

Rationale: The number of patients with coronary heart disease, including myocardial infarction, is increasing and novel therapeutic strategy is awaited. Tumor suppressor protein p53 accumulates in the myocardium after myocardial infarction, causes apoptosis of cardiomyocytes, and plays an important role in the progression into heart failure.

Objectives: We investigated the molecular mechanisms of p53 accumulation in the heart after myocardial infarction and tested whether anti-p53 approach would be effective against myocardial infarction.

Methods and Results: Through expression screening, we found that CHIP (carboxyl terminus of Hsp70-interacting protein) is an endogenous p53 antagonist in the heart. CHIP suppressed p53 level by ubiquitinating and inducing proteasomal degradation. CHIP transcription was downregulated after hypoxic stress and restoration of CHIP protein level prevented p53 accumulation after hypoxic stress. CHIP overexpression in vivo prevented p53 accumulation and cardiomyocyte apoptosis after myocardial infarction. Promotion of CHIP function by heat shock protein (Hsp)90 inhibitor, 17-allylamino-17-demethoxy geldanamycin (17-AAG), also prevented p53 accumulation and cardiomyocyte apoptosis both in vitro and in vivo. CHIP-mediated p53 degradation was at least one of the cardioprotective effects of 17-AAG.

Conclusions: We found that downregulation of CHIP level by hypoxia was responsible for p53 accumulation in the heart after myocardial infarction. Decreasing the amount of p53 prevented myocardial apoptosis and ameliorated ventricular remodeling after myocardial infarction. We conclude that anti-p53 approach would be effective to treat myocardial infarction. (*Circ Res*. 2010;106:1692-1702.)

Key Words: myocardial infarction ■ CHIP ■ p53 ■ hypoxia

The number of patients with coronary heart disease has been increasing and cardiovascular diseases are the leading cause of deaths in the Western world. Despite the development of pharmacological and nonpharmacological interventions, 33% of the men and 43% of the women die within 5 years after myocardial infarction (MI).[1] Therefore, a novel therapeutic approach against coronary heart disease is awaited.

Apoptosis of cardiomyocytes is accompanied with acute coronary occlusion.[2] Because apoptotic loss of cardiomyocytes causes heart failure,[3] inhibition of apoptosis has been suggested as an additional therapeutic approach to coronary heart disease.[4] In mice, overexpression of antiapoptotic Bcl-2 protein or genetic deletion of proapoptotic Bax protein have been reported to prevent apoptosis and reduce infarct size,[5–8] implicating that antiapoptotic approach is effective for prevention of ventricular remodeling after myocardial infarction.

The tumor suppressor *p53* is an important transcription factor that regulates cell cycle progression, cellular senescence, and apoptosis. Under physiological condition, p53 protein level is maintained low, but is elevated when cells are stressed or damaged.[9] The mechanism for keeping p53 protein level low involves several E3 ubiquitin ligases such as MDM2,[10,11] COP1,[12] and Pirh2.[13] Importantly, the expression of these proteins were positively regulated by p53, suggesting the role for negative-feedback loop against p53 elevation.

Protein level of p53 is also kept low in the heart but it is elevated when cardiac cells are exposed to hypoxia.[14–16]

Original received December 4, 2009; revision received April 6, 2010; accepted April 12, 2010.

From the Department of Cardiovascular Science and Medicine (A.T.N., S.O., T. Minamino, K.I., M.-L.L., T.S., S.N., H.A., T.N., I.S., I.K.), Chiba University Graduate School of Medicine, Japan; Department of Cardiovascular Medicine (A.T.N., H.A., I.S., I.K.), Osaka University Graduate School of Medicine, Japan; PRESTO (T. Minamino), Japan Science and Technology Agency, Saitama, Japan; and Laboratory for Alzheimer's Disease (N.S., T. Mizoroki, A.T.). RIKEN Brain Science Institute, Saitama, Japan.

This manuscript was sent to Junichi Sadoshima, Consulting Editor, for review by expert referees, editorial decision, and final disposition.

Correspondence to Issei Komuro, MD, PhD, Department of Cardiovascular Science and Medicine, Chiba University Graduate School of Medicine, 1-8-1 Inohana, Chuo-ku, Chiba, Japan. E-mail komuro-tky@umin.ac.jp

Circulation Research **is available at http://circres.ahajournals.org** **DOI: 10.1161/CIRCRESAHA.109.214346**

We have recently reported that elevation of p53 causes the development of pressure overload-induced heart failure.[16] We have also observed the elevation of p53 protein levels after myocardial infarction and shown that *p53* gene deletion improved cardiac function after myocardial infarction,[16] suggesting that the inhibition of p53 might become a novel therapeutic strategy for ischemic heart diseases.

As an initial approach for the investigation of anti-p53 therapy, we searched for an endogenous p53 antagonist in the heart. Through expression screening, we found that CHIP (carboxyl terminus of Hsp70-interacting protein) is an endogenous p53 antagonist that keeps p53 level low in the heart. We also found that CHIP downregulation is involved in the mechanism of p53 accumulation in the heart after myocardial infarction. Facilitating CHIP-mediated p53 degradation prevented apoptosis of cardiomyocytes and ameliorated ventricular remodeling in the postinfarct heart. The present study revealed the mechanism of p53 accumulation in the heart after myocardial ischemia and suggested that anti-p53 approach would be effective to treat myocardial infarction.

Non-standard Abbreviations and Acronyms	
17-AAG	17-allylamino-17-demethoxy geldanamycin
CHIP	carboxyl terminus of Hsp70-interacting protein
HIF	hypoxia-inducible factor
HRE	hypoxia-responsive element
Hsp	heat shock protein
HW/BW	heart weight/body weight
MI	myocardial infarction
PARP	poly(ADP-ribose)polymerase
siRNA	small interfering RNA

Methods

Expression Cloning

Expression cloning was performed as described previously[17] using PG13-Luc (kind gift from B. Vogelstein, Ludwig Center for Cancer Genetics and Therapeutics, Howard Hughes Medical Institute, and Sidney Kimmel Cancer Center, Johns Hopkins Medical Institutions, Baltimore, Md) as a reporter plasmid. Initially, cDNA expression library from human heart (Invitrogen) was separated into small pools that contain ≈100 clones each. cDNA clones that downregulate PG13 activity were isolated by sib-selection.

Cell Culture

COS7 and HEK293 cells are from ATCC and cultured in DMEM containing 10% FBS (Invitrogen). Neonatal rat cardiomyocytes were isolated from 1-day-old Wistar rats and cultured as described previously.[18] Cardiomyocytes were exposed to hypoxic stress by culturing under $CoCl_2$ or by culturing in hypoxic chamber (<1% O_2; Po_2, 18 to ≈20 mm Hg).

Animals

All protocols were approved by Chiba University review board. CHIP knockout mice and cardiac-specific inducible hypoxia-inducible factor (HIF)-1 knockout mice were described.[16,19,20] Heterozygous CHIP knockout mice were used in this study because homozygous knockout mice were perinatally lethal.[20] Cardiac-specific CHIP transgenic mice were generated by pronuclear injection of αMHC-HA-CHIP transgene construct. Coronary artery ligation was performed on 10-week old male mice as described previously.[21]

Statistical Analysis

Data are expressed as means±SE. The significance of differences among means was evaluated using analysis of variance (ANOVA), followed by Fisher's protected least significant difference test and Dunnett's test for multiple comparisons. Significant differences were defined as $P<0.05$.

Results

Identification of CHIP As a Novel p53 Antagonist From Heart cDNA Library

To elucidate novel p53 antagonists in the heart, we performed expression screening by expressing cDNA pools in COS7 cells together with a reporter plasmid, PG13-luciferase, which contains 13 copies of p53 binding site upstream of luciferase gene and responsive to wild-type p53 dependent transcription. From the screening of 500 cDNA pools, each containing around 100 individual cDNA clones obtained from human heart cDNA library, we found 5 pools that suppress the PG13 activity. Individual cDNA clone that downregulates the PG13 activity was identified by sib-selection. One of the molecules that was highly expressed in the heart (Figure I, A, in the Online Data Supplement, available at http://circres.ahajournals.org) was CHIP (also called STUB1 [Stip1 homology and U-box containing protein]), a chaperone-interacting protein with E3 ubiquitin ligase activity.[22] Transfection of CHIP suppressed endogenous and exogenous (by overexpression of p53) PG13 activity (Figure 1A) and decreased the protein levels of p53 (Figure 1B) in a plasmid dose-dependent manner in COS7 cells. Direct interaction between CHIP and p53 was confirmed both at the exogenous level in COS7 cells (Online Figure I, B) and at the endogenous level in cardiomyocytes (Online Figure I, C). Western blotting using anti-ubiquitin antibody after immunoprecipitation with p53 revealed that overexpression of CHIP increased poly-ubiquitinated p53 (which appears as a smear) (Online Figure I, D). The proteasomal inhibitor MG132 restored p53 protein level that was suppressed by CHIP (Online Figure I, E), indicating that CHIP directs p53 for proteasome-mediated degradation. When CHIP was knocked down in cardiomyocytes using small interfering (si)RNA, p53 expression was upregulated (Figure 1C), and p53 protein levels following CHIP knockdown were comparable to those induced by the knockdown of MDM2, a well known E3 ubiquitin ligase for p53 (Figure 1D). CHIP protein level was not changed by knockdown of MDM2 (Figure 1D). p53 protein levels were also markedly elevated in the heart of CHIP heterozygous mice (Figure 1E). These results suggest that CHIP induces degradation of wild-type p53 protein in cardiomyocytes, which is consistent with previous reports in other cells (H1299 cells and U2OS cells).[23,24] In addition, we revealed that CHIP is a crucial negative regulator that keeps p53 protein levels low in the heart under physiological conditions.

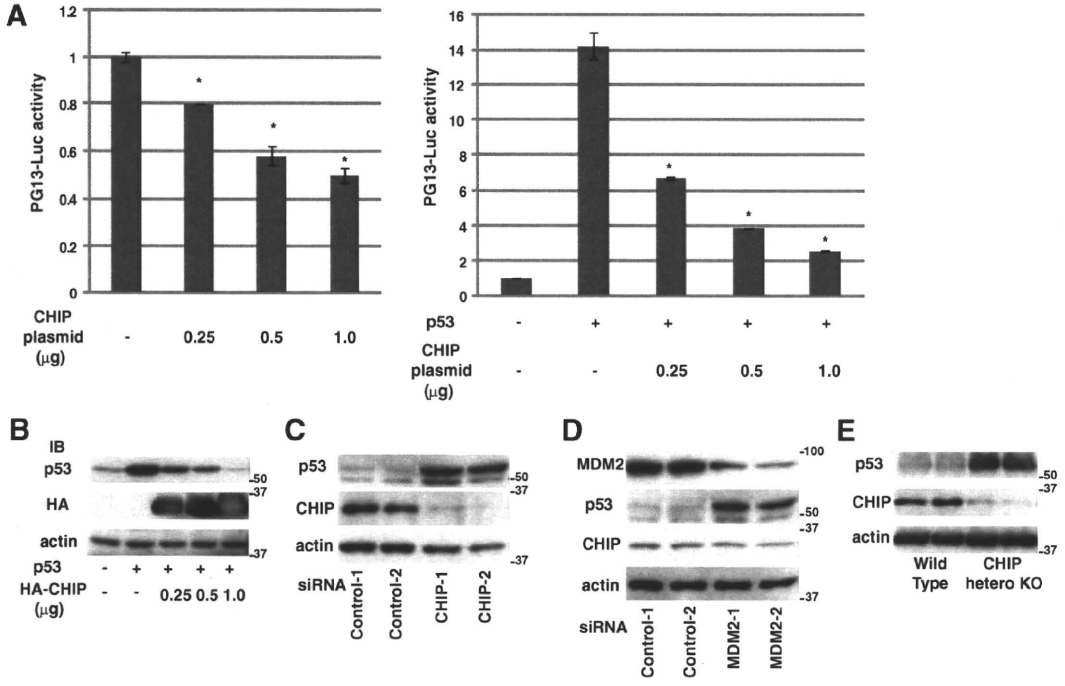

Figure 1. CHIP is a crucial negative regulator of p53 expression in the heart. A, Transfection of CHIP expressing plasmid suppressed endogenous **(left)** and exogenous **(right)** p53 transcriptional activity. *$P<0.01$ vs control; n=5. **B,** CHIP decreases p53 protein levels in COS7 cells. IB indicates immunoblot. **C,** p53 expression is upregulated by CHIP knockdown in cardiomyocytes. siRNAs specific to CHIP (CHIP-1 and CHIP-2), or control siRNA were transfected into cultured cardiomyocytes and protein levels of CHIP and p53 were examined by Western blotting. CHIP-1 and CHIP-2 represent 2 different siRNAs against CHIP. Control-1 is a commercially available control RNA, and control-2 is a scrambled control RNA. **D,** p53 upregulation is also observed by MDM2 knockdown. siRNAs specific to MDM2 (MDM2–1 and MDM2–2) or control siRNA were transfected into cultured cardiomyocytes, and protein levels of CHIP, p53, and MDM2 were examined by Western blotting. The extent of p53 upregulation by MDM2 knockdown was comparable to that induced by CHIP knockdown. **E,** Total protein of wild-type and CHIP heterozygous mice were analyzed by Western blotting. p53 expression is upregulated in the heart of CHIP heterozygous mice.

Molecular Mechanisms of Hypoxia-Induced p53 Accumulation

As CHIP regulates p53 status in the heart, we speculated that CHIP might be involved in the molecular mechanism of hypoxia-induced p53 accumulation in the heart. Cobalt chloride ($CoCl_2$) increases HIF-1 activity through preventing HIF-1α protein degradation and is widely used as a hypoxia mimicking reagent.[25,26] Treatment of cardiomyocytes with $CoCl_2$ (250 μmol/L) increased p53 protein level with a marked downregulation of CHIP protein level (Figure 2A). Notably, the expression of MDM2 was rather increased in this experimental condition. Because transcriptional regulation of MDM2 is known to be upregulated by p53 as a part of negative-feedback loop, increased MDM2 expression after $CoCl_2$ treatment may possibly be attributable to this feedback system against p53 elevation. Accumulation of p53 and downregulation of CHIP were also observed when cardiomyocytes were cultured in hypoxic chamber for 24 hours (Online Figure I, F). We confirmed that both treatments increased nuclear HIF-1α protein that binds to HIF-1α binding oligonucleotide by commercially available ELISA system (Online Figure I, G). We also analyzed the expression of p53 and CHIP in the heart after MI. p53 protein levels were increased on day 1 after MI and remained upregulated thereafter, whereas expression levels of CHIP were markedly downregulated on day 1, and remained at lower levels than those of controls (Figure 2B and analyzed in Online Figure II, A and B). In contrast, MDM2 protein levels were slightly increased after MI (Figure 2B). The inverse correlation between CHIP and p53 protein level implies the possible involvement of CHIP downregulation in the initiation of p53 accumulation after acute hypoxic stress. Other E3 ubiquitin ligases whose transcription is regulated by p53, such as MDM2, might work to reverse p53 level after initial accumulation of p53 as a feedback system to prevent further detrimental effects that might be elicited by chronic p53 elevation.

To investigate why CHIP is downregulated after hypoxic insult, we tested whether HIF-1 mediates hypoxia-induced downregulation of CHIP, because HIF-1 is known to downregulate some of its target genes through hypoxia-responsive element (HRE).[27–30] Human CHIP promoter (from −329 bases upstream of transcription start site to +39 bases downstream of transcription start site) that contains a conserved HRE at −49 (Figure 2C) was cloned upstream of luciferase reporter gene (pGL4-CHIP). pGL4-CHIP activity was significantly suppressed by both $CoCl_2$ treatment (24 hours) and HIF-1α overexpression in COS7 cells (Figure 2D). When a mutation was introduced into HRE at −49 (pGL4-CHIP-mutHRE), the luciferase activity was no longer responsive to hypoxic stress or HIF-1α overexpression (Figure 2D), suggesting that *CHIP* gene expression is downregu-

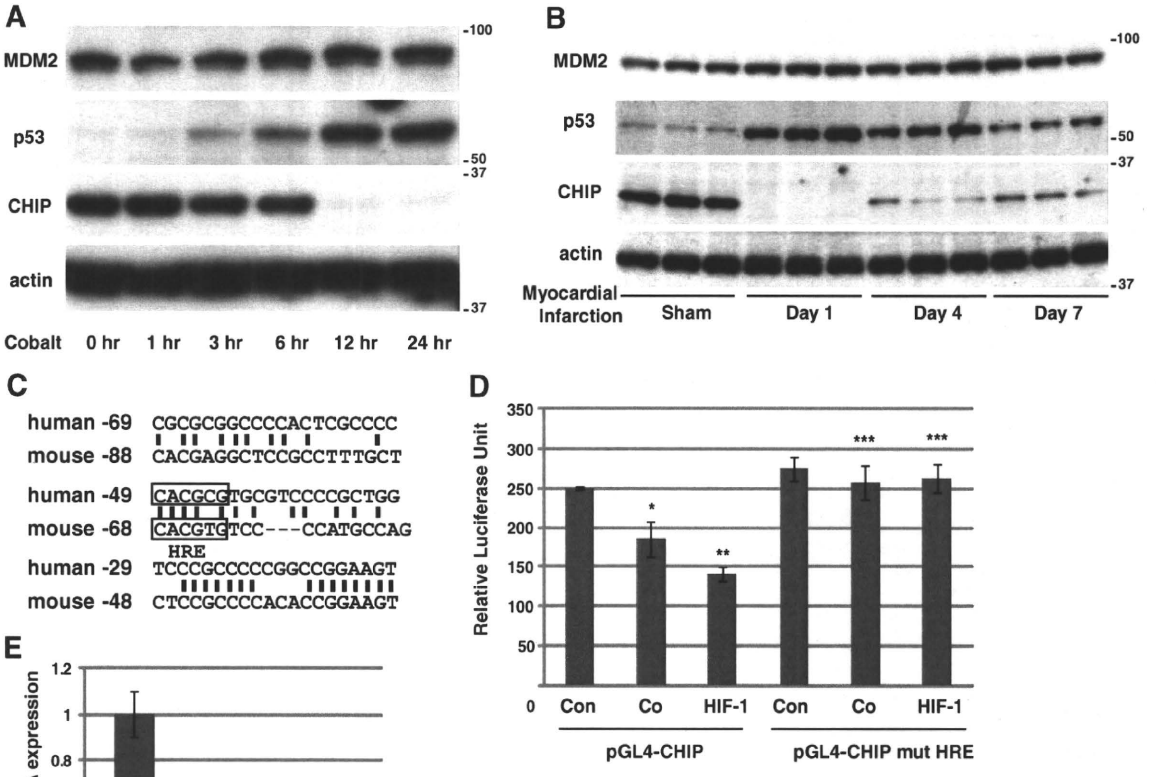

Figure 2. CHIP is downregulated by hypoxic stress. A, $CoCl_2$-induced p53 accumulation is associated with CHIP downregulation in cardiomyocytes. Cardiomyocytes were treated with 250 μmol/L $CoCl_2$, and protein was extracted at the indicated time point. **B,** Experimental myocardial infarction was created by permanent ligation of the coronary artery. Protein samples were extracted from total heart at the indicated time point after coronary artery ligation. CHIP expression is downregulated and p53 expression is upregulated after MI. **C,** Sequence comparison of human and mouse CHIP promoter. **Boxes** indicate conserved HRE. **D,** CHIP promoter activity is downregulated by $CoCl_2$ treatment and HIF-1α overexpression, and mutations (CACGTG to CTGGCG) introduced into HRE at −49 abrogated this response. CHIP promoter sequence from human genomic DNA (−329 to +39 from transcription start site) was cloned upstream of luciferase gene. Mutation was introduced using a kit from Stratagene. Luciferase assay was performed 24 hours after $CoCl_2$ treatment or HIF-1α overexpression. $^*P<0.05$, $^{**}P<0.01$, $^{***}P$=NS vs control; n=5. **E,** Real-time PCR analysis revealed mRNA level of CHIP was also downregulated by hypoxic stress (Co) and HIF-1α overexpression. RNA was extracted 24 hours after $CoCl_2$ treatment or HIF-1α overexpression. $^*P<0.01$.

lated by HIF-1 at the transcriptional level through HRE. Real-time PCR analysis revealed that exposure of cardiomyocytes to $CoCl_2$ (24 hours) and adenoviral overexpression of constitutively active HIF-1α led to marked downregulation of CHIP mRNA levels (Figure 2E), further supporting our data that hypoxic stress downregulates CHIP levels. HIF-1α gene is both required and sufficient for hypoxic stress-induced CHIP downregulation and p53 accumulation because knockdown of HIF-1α attenuated the effects of $CoCl_2$ treatment on expressions of p53 and CHIP (Online Figure III, A), and overexpression of constitutively active HIF-1α suppressed CHIP expression and increased p53 expression in cardiomyocytes (Online Figure III, B). Furthermore, downregulation of CHIP protein levels after MI was attenuated in cardiac-specific inducible HIF-1α conditional knockout mice[16] (Online Figure III, C). Collectively, these findings suggest that CHIP transcription is directly downregulated by hypoxia through HIF-1.

CHIP Protects Cardiomyocytes From Hypoxia-Induced p53-Mediated Apoptosis of Cardiomyocytes

Because hypoxia or p53 overexpression induces apoptotic cell death in cultured cardiomyocytes,[14] we next examined whether hypoxia-induced cardiomyocyte apoptosis is mediated by the HIF-1-CHIP-p53 pathway. $CoCl_2$ treatment (24 hours) induced p53 accumulation and promoted apoptosis of cardiomyocytes as assessed by cleaved poly (ADP-ribose) polymerase (PARP) expression (Figure 3A), Annexin V staining (Figure 3B and 3C), and caspase-3 activity (Figure 3D). $CoCl_2$-induced apoptosis was p53-dependent, because knockdown of p53 in $CoCl_2$-treated cardiomyocytes attenuated hypoxia-induced cell death (Figure 3A through 3D). We next assessed whether overexpression of CHIP could rescue $CoCl_2$-induced apoptosis. Adenovirus-mediated overexpression of CHIP in cardiomyocytes markedly downregulated p53 expression and attenuated apoptosis in $CoCl_2$-treated

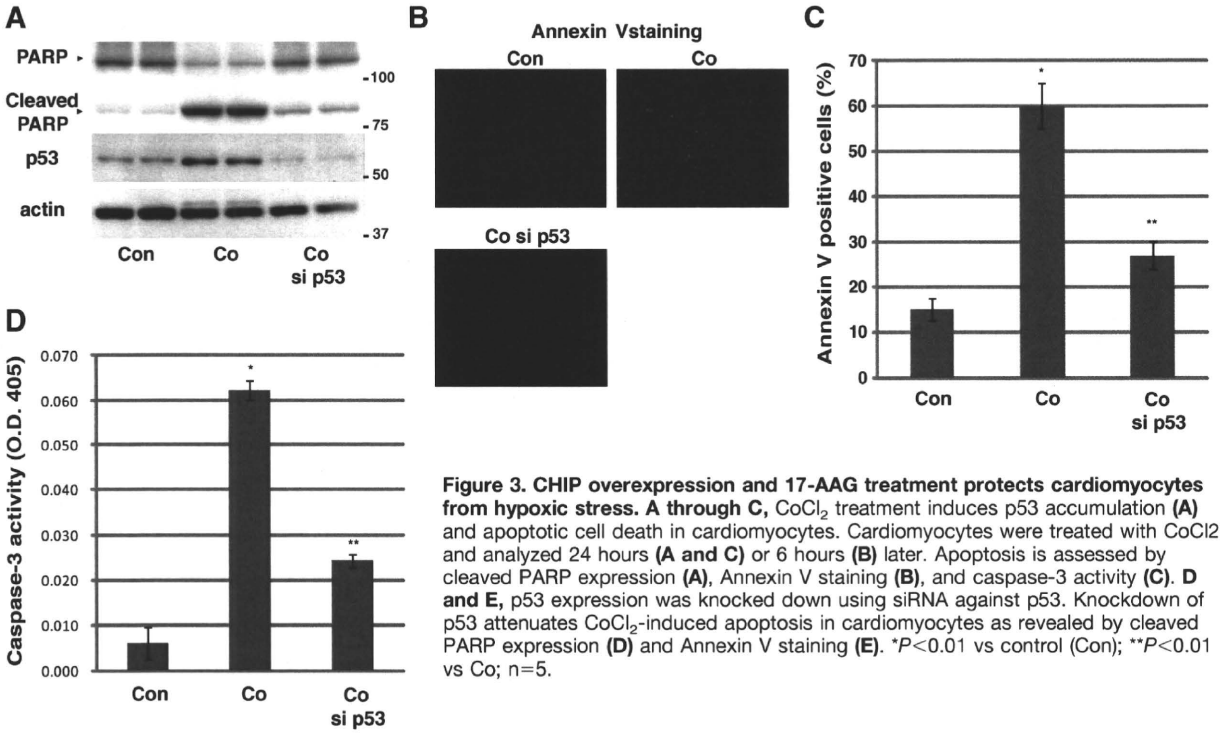

Figure 3. CHIP overexpression and 17-AAG treatment protects cardiomyocytes from hypoxic stress. A through C, $CoCl_2$ treatment induces p53 accumulation **(A)** and apoptotic cell death in cardiomyocytes. Cardiomyocytes were treated with CoCl2 and analyzed 24 hours **(A and C)** or 6 hours **(B)** later. Apoptosis is assessed by cleaved PARP expression **(A)**, Annexin V staining **(B)**, and caspase-3 activity **(C)**. **D and E,** p53 expression was knocked down using siRNA against p53. Knockdown of p53 attenuates $CoCl_2$-induced apoptosis in cardiomyocytes as revealed by cleaved PARP expression **(D)** and Annexin V staining **(E)**. *$P<0.01$ vs control (Con); **$P<0.01$ vs Co; n=5.

cardiomyocytes (Figure 4A through 4C). These results underscore our hypothesis that downregulation of CHIP is responsible for p53 accumulation after hypoxic stress. Moreover, forced expression of CHIP prevented hypoxia-induced cardiomyocyte apoptosis by inducing degradation of p53, suggesting that CHIP-mediated p53 degradation is a potential therapeutic target.

17-AAG Protects Cardiomyocytes From Hypoxia-Induced Apoptosis

Inhibitors for heat shock protein (Hsp)90 have been shown to promote proteasomal degradation of CHIP client proteins and to be effective for the diseases caused by the accumulation of CHIP substrates.[31,32] We therefore examined whether an Hsp90 inhibitor 17-allylamino-17-demethoxy geldanamycin (17-AAG) induces degradation of p53 protein and protects cardiomyocytes from hypoxic stress. In cardiomyocytes treated with $CoCl_2$, 17-AAG downregulated p53 expression (Figure 4D). 17-AAG treatment also suppressed hypoxia-induced cardiomyocyte apoptosis in a CHIP-dependent manner, because CHIP knockdown attenuated the protective effects of 17-AAG (Figure 4E through 4G). These results suggest that 17-AAG protects cardiomyocytes from hypoxic stress by promoting CHIP-mediated p53 degradation.

Interestingly, protein level of CHIP was increased by 17-AAG treatment (Figure 4E). As mRNA level of CHIP was not changed by 17-AAG treatment (Online Figure IV, A), we speculated that protein stability was affected by 17-AAG treatment. When protein translation was inhibited by cycloheximide, 17-AAG treatment dramatically extended the protein half-life of CHIP (Online Figure IV, B and C). 17-AAG also upregulated the protein stability of other proteins, Hsp70 and HSF-1 (Online Figure IV, B and C). Because 17-AAG exerted some antiapoptotic effects even in the cells of negligible CHIP protein level (Figure 4E and 4F), upregulation of these cardioprotective proteins[33,34] might mediate part of the effects of 17-AAG. It remains to be determined how 17-AAG prolongs protein half-life of certain kinds of proteins.

CHIP and 17-AAG Prevent Apoptosis and Ventricular Remodeling After Myocardial Infarction

We next examined whether promotion of CHIP-mediated p53 degradation could attenuate ischemic cardiac injury also in vivo. For this purpose, transgenic mice which overexpress CHIP specifically in the heart (CHIP-Tg) (Figure 5A) were subjected to permanent coronary artery ligation. In CHIP-Tg mice, elevation of p53 protein levels (Figure 5B) and apoptotic cardiomyocyte death in the border zone of the infarct area (Figure 5B and 5C) were attenuated compared to wild-type littermates at 24 hours after the MI operation. Apoptotic death of the cardiomyocytes in the remote zone of the infarct was not changed between littermates (data not shown). We next examined whether this decrease in apoptotic cell death leads to attenuation of cardiac ventricular remodeling. At day 14, CHIP-Tg mice exhibited smaller heart weight/body weight (HW/BW) ratio, better contractility and less ventricular remodeling (Figure 5D and 5E) compared to wild-type littermates. These results provides an evidence for our hypothesis that CHIP downregulation is responsible for p53 accumulation after myocardial infarction, and suggests that CHIP overexpression is protective for the heart by preventing p53 accumulation and cardiomyocyte apoptosis after myocardial infarction.

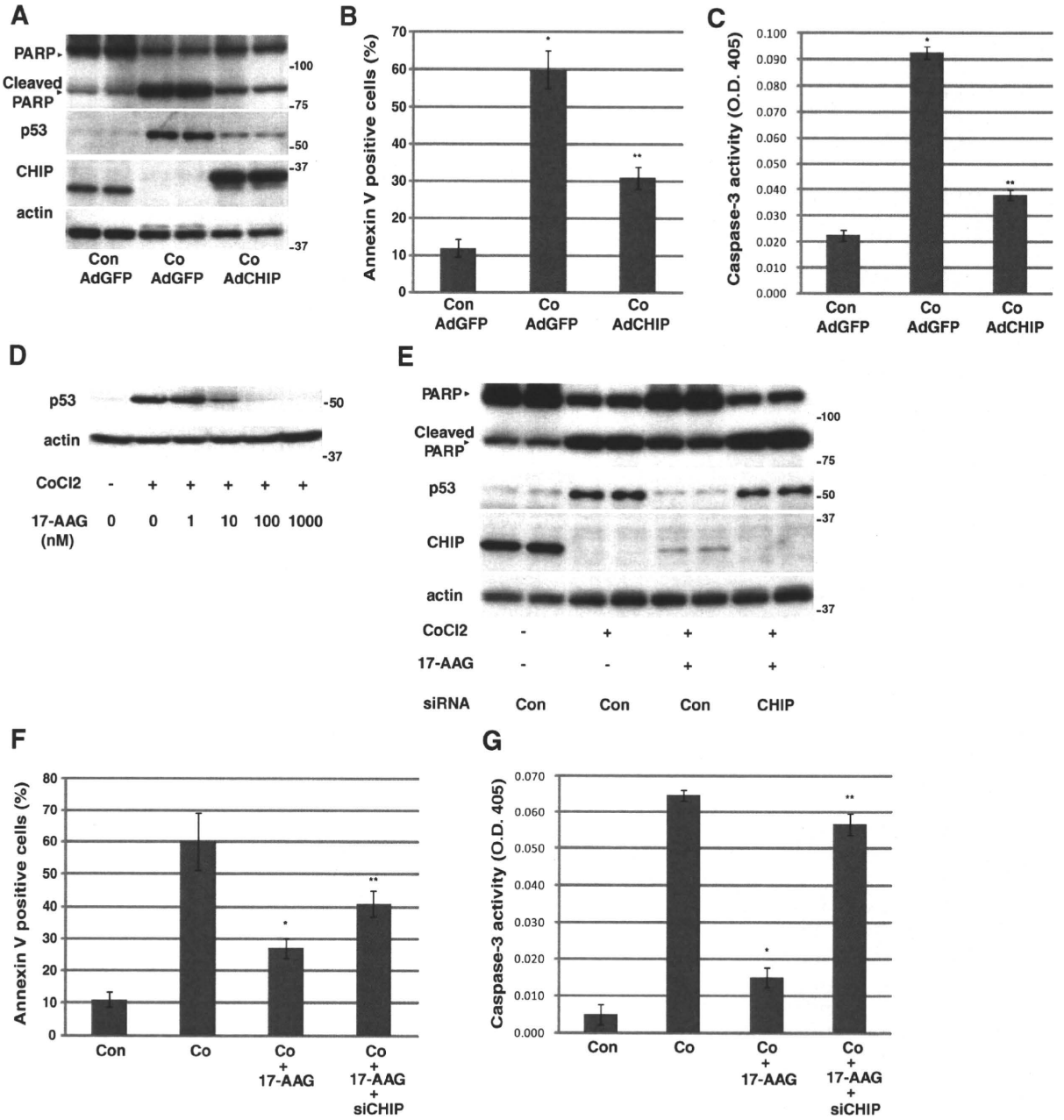

Figure 4. Promoting CHIP-mediated p53 degradation is protective against hypoxic stress. A through C, Overexpression of CHIP attenuates $CoCl_2$-induced p53 accumulation **(A)** and apoptosis in cardiomyocytes. Cardiomyocytes were infected with adenovirus harboring green fluorescent protein (GFP) or CHIP. Twenty-four hours later, culture medium was changed and the cells were treated with $CoCl_2$. Apoptosis was assessed by cleaved PARP expression **(A)**, Annexin V staining **(B)**, and caspase-3 activity **(C)**. *$P<0.01$ vs control (Con)+AdGFP; **$P<0.01$ vs Co+AdGFP; n=5. **D,** 17-AAG downregulates p53 expression in cardiomyocytes. Neonatal rat cardiomyocytes were treated with $CoCl_2$ with or without 17-AAG at the indicated concentration. **E through G,** 17-AAG inhibits $CoCl_2$-induced p53 accumulation **(E)** and apoptosis in cardiomyocytes, which is abrogated by CHIP knockdown. Neonatal rat cardiomyocytes were transfected with control siRNA or siRNA against CHIP. Twenty-four hours later, medium was changed and the cells were treated with $CoCl_2$ and/or 17-AAG. Apoptosis is assessed by cleaved PARP expression **(E)**, Annexin V staining **(F)**, and caspase-3 activity **(G)**. *$P<0.01$ vs Co; **$P<0.05$ vs Co +17-AAG; n=3.

We also examined whether treatment with 17-AAG exerts similar cardioprotective effects. 17-AAG (10 mg/kg) or vehicle was intraperitoneally injected immediately after permanent coronary artery ligation. This single injection of 17-AAG effectively suppressed the elevation of p53 protein levels and apoptotic cell death in the border zone of the infarct area at 24 hours after the operation (Figure 6A and 6B). As p53 protein level was kept elevated even 4 and 7 days after MI (Figure 2B), 17-AAG was injected every other days and we assessed whether 17-AAG treatment also leads to attenuation of ventricular remodeling, as observed in CHIP-Tg mice. At day 14, mice treated with 17-AAG exhibited smaller HW/BW ratio, better contractility,

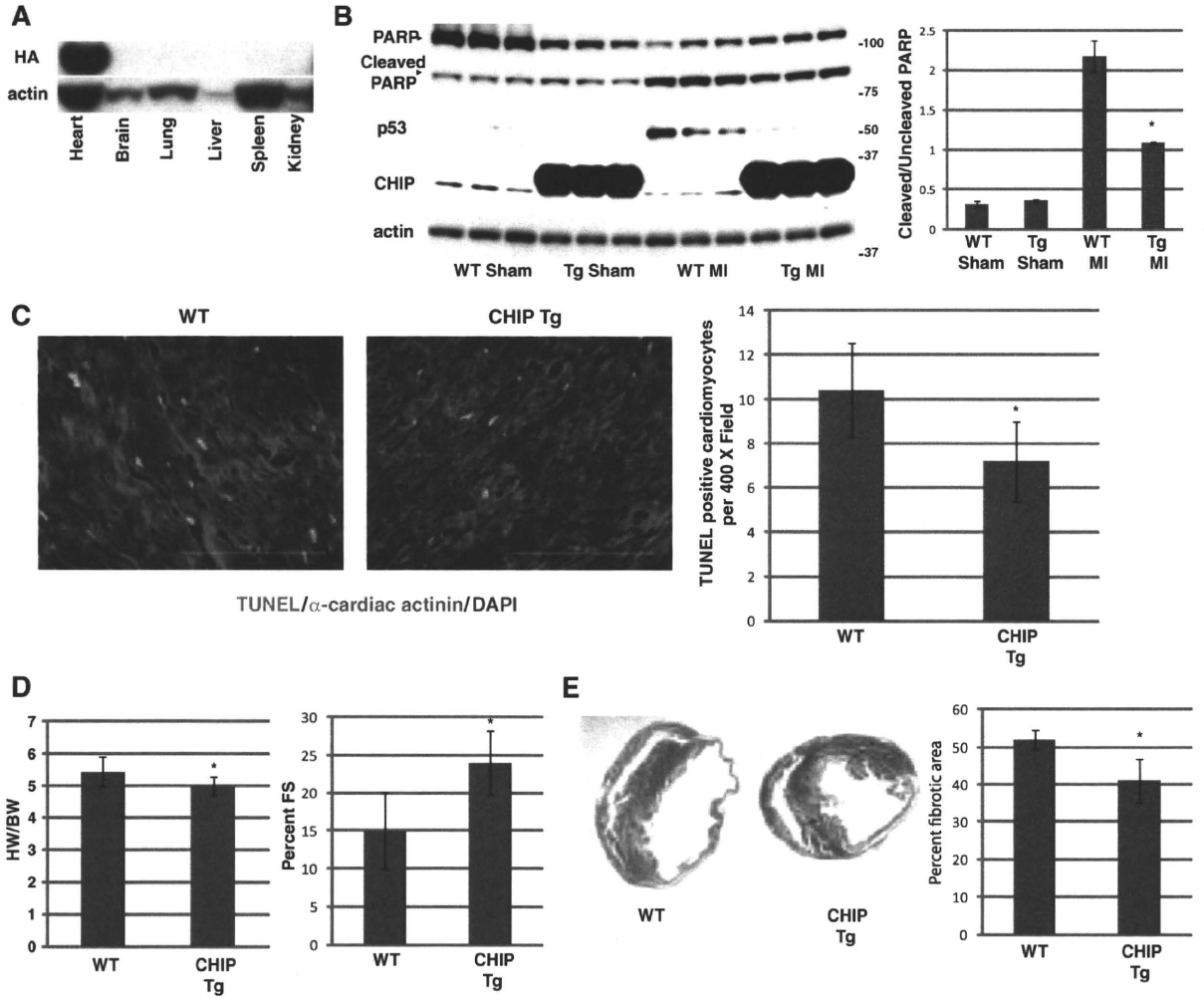

Figure 5. Overexpression of CHIP attenuates ischemic cardiac injury in vivo. A, Cardiac-specific expression of HA-tagged human CHIP in CHIP-Tg mice. **B and C,** p53 accumulation **(B)** and apoptosis 1 day after MI are reduced in CHIP-Tg mice. Apoptosis was assessed by cleaved PARP expression **(B)** and TUNEL staining **(C)**. Cleaved PARP level was assessed by densitometric analysis on band intensity of cleaved PARP over uncleaved PARP. $P<0.05$ vs WT; n=3. WT indicates wild-type mice. **D and E,** Postinfarct cardiac remodeling is attenuated in CHIP-Tg mice (n=15). HW/BW ratio **(D, left)**, contractile function **(D, right)**, and percentage fibrotic area **(E)**. *$P<0.01$ vs WT (n=30).

and less ventricular remodeling (Figure 6C and 6D). Interestingly, the effects of 17-AAG were greater than CHIP overexpression (compare Figures 5 and 6), suggesting that 17-AAG possesses cardioprotective activities that do not involve CHIP-mediated p53 degradation. As protein stability of cardioprotective proteins such as Hsp70 and HSF-1 was increased in vitro (Online Figure IV, B and C), we have examined the expression of these proteins in 17-AAG–treated mice. As expected, expression of these two proteins were increased by 17-AAG treatment (Online Figure IV, D), indicating that 17-AAG exerts its antiapoptotic effects by at least two mechanisms, one by inducing CHIP-mediated p53 degradation and the other by increasing cardioprotective heat shock proteins.

Finally, we examined the contribution of CHIP-mediated p53 degradation on the cardioprotective effects of 17-AAG. For that purpose we used CHIP heterozygous mice. There were no differences in cleaved PARP level (Figure 7A; compare WT Sham and Het Sham) or cardiac function between CHIP heterozygous mice and wild-type littermates at the basal level (Table). Following coronary artery ligation, however, apoptotic cell death was observed more prominently in CHIP heterozygous mice as assessed by increased cleaved PARP level (Figure 7A; compare WT MI and Het MI) and increased TUNEL positive cells (Figure 7B). The level of p53 accumulation was comparable following myocardial infarction between wild-type and CHIP heterozygous mice, suggesting the presence of p53 independent mechanisms for enhanced apoptosis caused by CHIP haploinsufficiency. Chronically, CHIP heterozygous mice showed worse cardiac function and worse ventricular remodeling compared with wild-type mice (Figure 7C and 7D). 17-AAG treatment was less effective to reduce p53 protein level, cleaved PARP level (Figure 7A; compare Het MI and Het MI 17-AAG), and TUNEL positive cardiomyocytes in CHIP heterozygous mice, possibly as a result of CHIP haploinsufficiency. 17-AAG treatment had minimal effects on improvements of cardiac function and ventricular remodeling on CHIP heterozygous mice also in the chronic phase (Figure 7C and 7D).

However, we must emphasize that the effects of 17-AAG were not fully attributable to CHIP-mediated p53 degradation

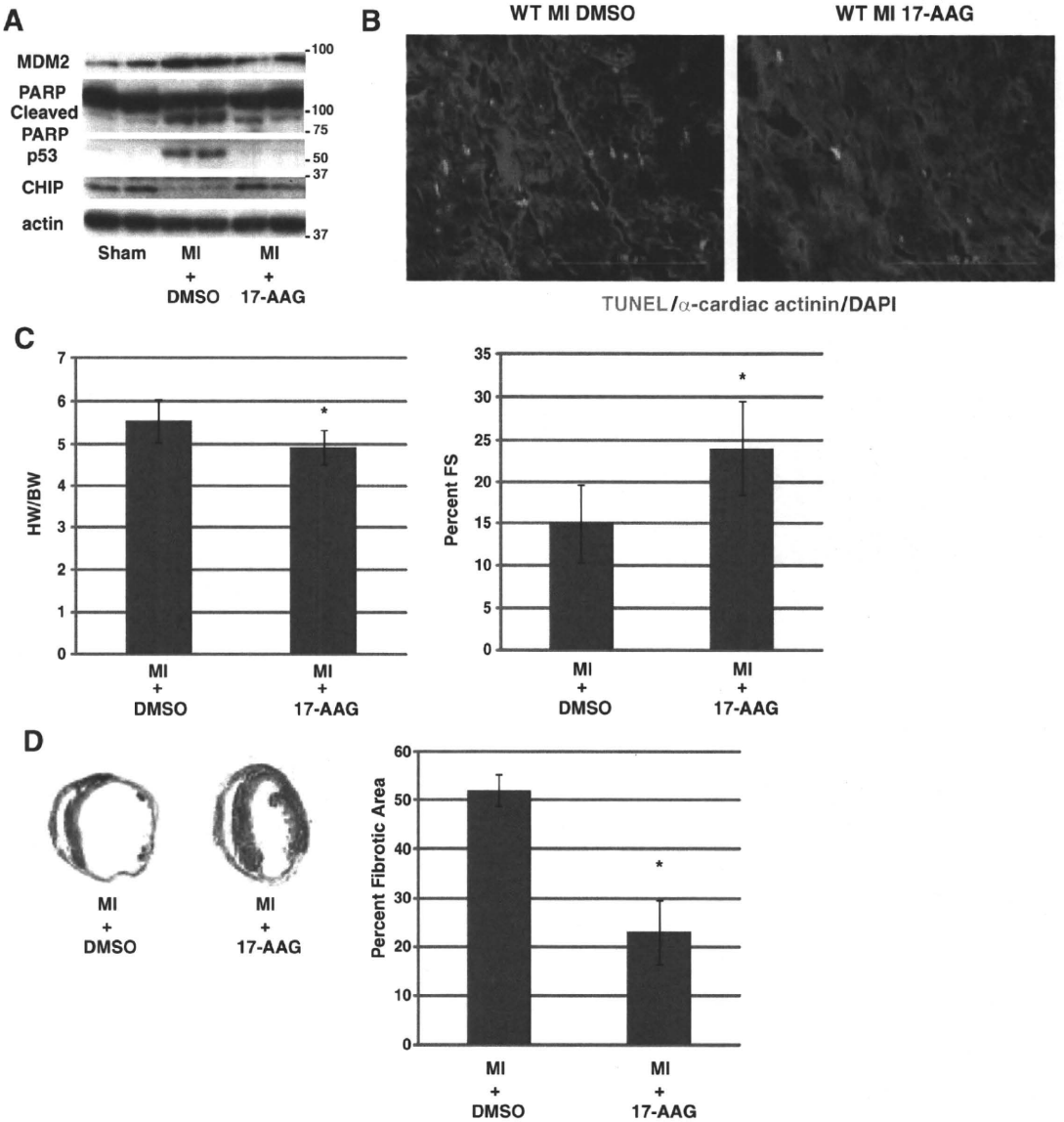

Figure 6. 17-AAG treatment attenuates ischemic cardiac injury in vivo. A, Accumulation of p53 and cleaved PARP in the heart after MI are reduced by 17-AAG treatment. 17-AAG (10 mg/kg) or vehicle was injected immediately after coronary ligation. **B,** Apoptotic cardiomyocytes at 1 day after MI was reduced in 17-AAG–treated mice. Apoptosis was assessed by TUNEL staining. **C and D,** Postinfarct cardiac remodeling is attenuated by 17-AAG treatment (n=20). HW/BW ratio **(C, left)**, contractile function **(C, right)**, and fibrotic area **(D)**. *$P<0.001$; vs MI+DMSO (n=30).

because upregulation of heat shock proteins by 17-AAG was also impaired in CHIP heterozygous mice (Figure 7A; compare WT MI 17-AAG and Het MI 17-AAG). Therefore, it would be fair to conclude that 17-AAG exerts multiple cardioprotective effects after myocardial infarction and at least one of its effects were mediated by promotion of CHIP-mediated p53 degradation.

Discussion

In the present study, we found that accumulation of p53 protein after myocardial ischemia is initiated by HIF-1 dependent downregulation of CHIP level. We have found that CHIP overexpression decreased the amount of p53 and prevented myocardial apoptosis and ameliorated ventricular remodeling after myocardial infarction. We have also found that Hsp90 inhibitor, 17-AAG, exerted similar antiapoptotic and cardioprotective effects after myocardial infarction and showed that these effects of 17-AAG was at least in part mediated by promotion of CHIP-mediated p53 degradation.

Although hypoxic stimuli have been reported to raise p53 protein levels in a variety of cell types, molecular mechanisms of p53 accumulation have been largely unknown. In the present study, we unveiled that downregulation of CHIP protein is critically involved in this process. We found that CHIP expression was downregulated after hypoxic stress through HIF-1–mediated suppression of *CHIP* promoter (Figure 2). We also found that overexpression of CHIP attenuated the p53 accumulation after hypoxic stress (Figures 4A and 5B). These results